PHILOSOPHICAL TRANSACTIONS OF THE ROYAL SOCIETY A MATHEMATICAL, PHYSICAL & ENGINEERING SCIENCES

On the Gortler Instability in Hypersonic Flows: Sutherland Law Fluids and Real Gas Effects

Yibin Fu, Philip Hall and Nicholas Blackaby

Phil. Trans. R. Soc. Lond. A 1993 **342**, 325-377
doi: 10.1098/rsta.1993.0025

On the Görtler instability in hypersonic flows: Sutherland law fluids and real gas effects†

By Yibin Fu, Philip Hall and Nicholas Blackaby

Department of Mathematics, University of Manchester, Oxford Road, Manchester M13 9PL, U.K.

Contents

The Görtler vortex instability mechanism in a hypersonic boundary layer on a curved wall is investigated in this paper. Our aim is to clarify the precise roles of the effects of boundary layer growth, wall cooling and gas dissociation in the determination of stability properties. We first assume that the fluid is an ideal gas

† This paper was produced from the authors' disk by using the TEX typesetting system.

Phil. Trans. R. Soc. Lond. A (1993) **342**, 325–377
Printed in Great Britain

with viscosity given by Sutherland's law. It is shown that when the free-stream Mach number M is large, the boundary layer divides into two sublayers: a wall layer of $O(M^{3/2})$ thickness (in terms of the boundary layer variable) over which the basic state temperature is $O(M^2)$, and a temperature adjustment layer of $O(1)$ thickness over which the basic state temperature decreases monotonically to its free-stream value. Görtler vortices which have wavelength comparable with the boundary layer thickness (i.e. have local wavenumber of order $M^{-3/2}$) are referred to as wall modes. We show that their downstream evolution is governed by a set of parabolic partial differential equations and that they have the usual features of Görtler vortices in incompressible boundary layers. As the local wavenumber increases, the neutral Görtler number decreases and the centre of vortex activity moves towards the temperature adjustment layer. Görtler vortices with wavenumber of order one or larger must necessarily be trapped in the temperature adjustment layer, and it is this mode which is the most dangerous. For this mode, we find that the leading-order term in the Görtler number expansion is independent of the wavenumber and is due to the curvature of the basic state. This term is also the asymptotic limit of the neutral Görtler numbers of the wall mode. To determine the higher-order correction terms in the Görtler number expansion, we have to distinguish between two wall curvature cases. When the wall curvature is proportional to $(2x)^{-3/2}$, where x is the streamwise variable, the Mach number M can be scaled out of the problem and the boundary layer growth takes place over an $O(1)$ lengthscale. The evolution properties of Görtler vortices are then similar to those in incompressible flows. In the more general case when the wall curvature is not proportional to $(2x)^{-3/2}$, the effect of the curvature of the basic state persists in the downstream development of Görtler vortices; non-parallel effects are important over a larger range of wavenumbers, and they become of second order only when the local wavenumber is of order higher than $O(M^{1/4})$. In the latter case the Görtler number expansion has the first two terms independent of non-parallel effects; the first term being due to the curvature of the basic state and the second term due to viscous effects. The second term becomes comparable with the first term when the wavenumber reaches the order $M^{3/8}$, in which case another correction term can also be found independently of non-parallel effects. Next we investigate real gas effects by assuming that the fluid is an ideal dissociating gas. We find that both gas dissociation and wall cooling are destabilizing for the mode trapped in the temperature adjustment layer, but for the wall mode trapped near the wall the effect of gas dissociation can be either destabilizing or stabilizing.

1. Introduction

This paper is an extension of our previous paper Hall & Fu (1989) on the linear development of Görtler vortices and the reader is referred to that paper for a more detailed review of the relevant literature. In that paper, we assumed that the fluid was an ideal gas with the viscosity given by Chapman's law. It was found that when a hypersonic boundary layer first loses stability to Görtler vortices, the vortices are necessarily trapped in the logarithmically thin temperature

PHILOSOPHICAL TRANSACTIONS OF THE ROYAL SOCIETY A MATHEMATICAL, PHYSICAL & ENGINEERING SCIENCES

adjustment layer over which the temperature of the basic flow changes rapidly to its free stream value. In other words, the mode trapped in the temperature adjustment layer has a smaller Görtler number than any other mode. As a consequence of this region of vortex activity being thin (which leads us to consider Görtler vortices of small wavelength), the perturbation equations governing the downstream development of the vortices reduce to ordinary differential equations within the order of approximation considered if the appropriate 'fast' streamwise dependence of the instability is built into the disturbance flow structure. Thus the non-uniqueness of the neutral stability curve associated with incompressible Görtler vortices disappears at high Mach numbers and a unique neutral curve with distinct left and right branches is obtained.

However, a real fluid has its viscosity given by the more complicated Sutherland's law. Although in most of the previous investigations on compressible boundary layers Chapman's viscosity law has been adopted as an approximation to Sutherland's law, such an approximation is poor for hypersonic flows in which the fluid temperature varies significantly across the boundary layer.† Thus it is of interest to investigate how our previous results are modified if the more realistic Sutherland's law is adopted. This is one of the problems which we are addressing in the present paper.

The other problems which we consider are the effects of gas dissociation and wall cooling on the flow stability. For a hypersonic boundary layer, the temperature near the wall is typically of order M^2 where M is the free stream Mach number, and gas dissociation must necessarily take place. Also, in practical situations, walls can not possibly withstand such high temperatures and they must be cooled. Thus it is also of special interest to clarify the precise roles of these two mechanisms in the stability properties of hypersonic boundary layers.

The major difference between Görtler vortices in incompressible and hypersonic flows is that the presence of the temperature adjustment layer at the edge of a hypersonic boundary layer where the basic temperature field decreases rapidly to its free-stream value enables hypersonic Görtler vortices to be concentrated well away from the wall. In the incompressible case we know from the work of Hall (1982, 1983), and Denier *et al.* (1990) that at order one Görtler numbers unstable Görtler vortices are not localized within the basic boundary layer. At higher Görtler number the most dangerous Görtler vortices have a wavelength small compared with the boundary layer thickness and are trapped near the wall. At order one Mach numbers this situation does not change significantly and the non-parallel problem has been discussed by Wadey (1993) and Spall & Malik (1989). In the latter two investigations the non-parallel equations were solved numerically following the approach of Hall (1983), the main result obtained was that the neutral position or growth rate of a Görtler vortex is a function of its upstream history. However, the numerical calculations of Wadey (1993) suggest that as the Mach number increases the position where an unstable Görtler vortex locates itself moves towards the edge of the boundary layer. That result is consistent with what we shall find in this paper.

† However, a referee has kindly pointed out to us that in some instances Chapman's Law is a good approximation. Thus for example the hypersonic Rayleigh mode instability problem discussed by Smith & Brown (1990) compares favourably with for example the calculations of Mack (1984), who used a combination of the Chapman's and Sutherland's laws.

PHILOSOPHICAL TRANSACTIONS OF THE ROYAL SOCIETY A MATHEMATICAL, PHYSICAL & ENGINEERING SCIENCES

The present paper is limited only to the linear régime of vortex growth; nonlinear aspects of incompressible or low Mach number Görtler vortex growth have been discussed by Hall (1988), and Wadey (1993). For a detailed account of the nonlinear régime the reader is referred to the review paper by Hall (1990). Before going on to discuss the work presented here we also note that hypersonic boundary layers are also susceptible to instabilities not induced by streamline curvature. Thus, for example, Smith (1989), Cowley & Hall (1990), Smith & Brown (1990), Blackaby *et al.* (1993) have discussed the role of Rayleigh or Tollmien–Schlichting wave instabilities in hypersonic boundary layers. In fact, as we shall see later, there are quite a few analogies between our results for Görtler instability and the results for Rayleigh instability given by these authors (e.g. the temperature adjustment layer is the most dangerous site for both instabilities). Therefore, any nonlinear investigation of Görtler vortices at hypersonic speeds must allow for the possible interaction of the vortices with other finite-amplitude instability mechanisms.

This paper is organized as follows. In § 2 and in the first part of § 3 we discuss the basic state. Here we discuss the significant changes in the basic state which occur when Sutherland's law is used instead of the Chapman law. In particular, the logarithmically thin temperature adjustment layer found for Chapman fluids is now replaced by a more complex adjustment layer of $O(1)$ thickness. We shall see later that this difference will strongly affect the downstream evolution properties of Görtler vortices.

In § 3 we formulate the linear stability problem for a hypersonic boundary layer and the linear perturbation equations are obtained in the usual manner by superimposing a Görtler vortex structure on the basic state and linearizing the Navier–Stokes equations. There are then two modes (as defined in the abstract) which need to be studied due to the layered structure of the basic state. We first investigate the mode of Görtler vortices which have wavelength comparable with the thickness of the temperature adjustment layer. When Chapman's law is used, the perturbation equations can be reduced to a set of ordinary differential equations after the wavelength of the vortices is scaled by the thickness of the logarithmically thin adjustment layer. However, here we show that because the temperature adjustment layer is of $O(1)$ thickness (in terms of the boundary layer variable) when Sutherland's law is used, non-parallel effects are more pronounced and their effects are different for different wall curvatures. To be more specific, when the wall curvature is proportional to $(2x)^{-3/2}$, the curvature of the basic state only gives rise to an $O(M^{3/2})$ wavenumber independent term in the Görtler number expansion and its effect is not present in the downstream development of Görtler vortices in the neighbourhood of the neutral position; while in the more general case when the wall curvature is not proportional to $(2x)^{-3/2}$, the curvature of the basic state not only gives rise to an $O(M^{3/2})$ wavenumber independent term in the Görtler number expansion, but it also affects the downstream evolution of Görtler vortices in the neighbourhood of the neutral position and thus affects the determination of other higher-order correction terms to the Görtler number expansion. Sections 4 and 5 are respectively devoted to the discussion of these two cases.

In § 4, we show that in the special curvature case $\kappa(x) = (2x)^{-3/2}$, the Mach number can be scaled out of the problem and the situation is then similar to that

PHILOSOPHICAL TRANSACTIONS OF THE ROYAL SOCIETY A MATHEMATICAL, PHYSICAL & ENGINEERING SCIENCES

in the incompressible flows. In the $O(1)$ wavenumber régime, the perturbation equations are partial differential equations and they have to be solved numerically by a marching procedure. We present our numerical results which show that neutral curves depend crucially on what initial perturbations we impose and where we impose them. In the large wavenumber limit, non-parallel effects are negligible and a simple asymptotic expression is obtained for the Görtler number in terms of the wavenumber. In § 5, we show that because of the persistent effect of the curvature of the basic state, non-parallel effects are important over a larger range of wavenumbers and they become negligible only when the wavenumber is of order larger than $O(M^{1/4})$. Thus for wavenumbers of order $O(M^{\alpha})$ with $\alpha \leq \frac{1}{4}$, the perturbation equations which govern the downstream evolution of Görtler vortices are partial differential equations and non-parallel effects are dominant. When $\alpha > \frac{1}{4}$, non-parallel effects are not so pronounced and the Görtler number expansion has the first two terms independent of non-parallel effects; the first term due to the curvature of the basic state and the second term due to viscous effects. The second term becomes comparable with the first term when the wavenumber reaches the order $O(M^{3/8})$, in which case another correction term can also be found independently of non-parallel effects.

To complete our stability analysis, we devote § 6 to the wall mode which has wavelength comparable with the boundary layer thickness. This mode is non-parallel and neutral curves have to be obtained by solving a set of partial differential equations. Our numerical results show that neutral curves, although non-unique, all decrease monotonically with the wavenumber and tend to a constant value in the large wavenumber limit, thus matching in the large wavenumber limit with the mode trapped in the temperature adjustment layer.

In § 7, we investigate real gas effects and wall cooling effects. We assume that the fluid is an ideal dissociating gas. After dissociation has taken place, the fluid becomes a gas mixture. We first determine the constitutive properties of the gas mixture and then show how our previous results for ideal gases are modified when gas dissociation is taken into account. We show for the mode trapped in the temperature adjustment layer that the leading-order Görtler number is decreased by both gas dissociation and wall cooling and thus we conclude that both these mechanisms are destabilizing. For the wall mode, neutral curves are not unique and so we cannot draw any general conclusion. For the case we consider, the neutral curves corresponding to the two models intersect, so the effect of gas dissociation can be either destabilizing or destabilizing. Finally in the last section we give some further discussion.

2. Basic state

Consider a hypersonic boundary layer over a rigid wall of variable curvature $(1/A)\kappa(x^*/L)$, where L is a typical streamwise lengthscale and A is a lengthscale characterizing the radius of curvature of the wall. We choose a curvilinear coordinate system (x^*, y^*, z^*) with x^* measuring distance along the wall, y^* perpendicular to the wall and z^* in the spanwise direction. The corresponding velocity components are denoted by (u^*, v^*, w^*) and density, temperature and viscosity by ρ^*, T^* and μ^* respectively. The free stream values of these quantities will be

PHILOSOPHICAL TRANSACTIONS OF THE ROYAL SOCIETY A MATHEMATICAL, PHYSICAL & ENGINEERING SCIENCES

signified by a subscript ∞. We define the Reynolds number R by

$$R = u^*_\infty L \rho^*_\infty / \mu^*_\infty, \tag{2.1}$$

and the Görtler number by

$$G = 2R^{1/2}(L/A). \tag{2.2}$$

The former is always assumed to be large, while the order of the latter will be shown to be a function of the Mach number. In the following analysis, coordinates (x^*, y^*, z^*) are scaled on $(L, R^{-1/2}L, R^{-1/2}L)$, the velocity (u^*, v^*, w^*) is scaled on $(u^*_\infty, R^{-1/2}u^*_\infty, R^{-1/2}u^*_\infty)$ and other quantities such as ρ^*, T^*, and μ^* are scaled on their free stream values with the only exception that the pressure p^* is scaled on $\rho^*_\infty u^{*2}_\infty$ and the bulk viscosity is scaled on μ^*_∞. All dimensionless quantities will be denoted by the same letters without a superscript $*$. Then after terms of relative order $1/R$ have been neglected, the Navier–Stokes equations become

$$\frac{\partial \rho}{\partial t} + \frac{\partial}{\partial x_\beta}(\rho v_\beta) = 0, \tag{2.3}$$

$$\rho \frac{\mathrm{D}u}{\mathrm{D}t} = -\frac{\partial p}{\partial x} + \frac{\partial}{\partial y}\left(\mu \frac{\partial u}{\partial y}\right) + \frac{\partial}{\partial z}\left(\mu \frac{\partial u}{\partial z}\right), \tag{2.4}$$

$$\begin{aligned}\rho \frac{\mathrm{D}v}{\mathrm{D}t} + \tfrac{1}{2}G\kappa u^2 = {} & -R\frac{\partial p}{\partial y} + \frac{\partial}{\partial y}\left\{(\lambda - \tfrac{2}{3}\mu)\frac{\partial v_\beta}{\partial x_\beta}\right\} + \frac{\partial}{\partial x_\beta}\left(\mu \frac{\partial v_\beta}{\partial y}\right) \\ & + \frac{\partial}{\partial y}\left(\mu \frac{\partial v}{\partial y}\right) + \frac{\partial}{\partial z}\left(\mu \frac{\partial v}{\partial z}\right),\end{aligned} \tag{2.5}$$

$$\begin{aligned}\rho \frac{\mathrm{D}w}{\mathrm{D}t} = {} & -R\frac{\partial p}{\partial z} + \frac{\partial}{\partial z}\left\{(\lambda - \tfrac{2}{3}\mu)\frac{\partial v_\beta}{\partial x_\beta}\right\} \\ & + \frac{\partial}{\partial x_\beta}\left(\mu \frac{\partial v_\beta}{\partial z}\right) + \frac{\partial}{\partial y}\left(\mu \frac{\partial w}{\partial y}\right) + \frac{\partial}{\partial z}\left(\mu \frac{\partial w}{\partial z}\right),\end{aligned} \tag{2.6}$$

$$\begin{aligned}\rho c_p \frac{\mathrm{D}T}{\mathrm{D}t} = {} & \mu(\gamma - 1)M^2\left[\left(\frac{\partial u}{\partial y}\right)^2 + \left(\frac{\partial u}{\partial z}\right)^2\right] \\ & + (\gamma - 1)M^2\left[1 - \rho\left(\frac{\partial h}{\partial p}\right)_T\right]\frac{\mathrm{D}p}{\mathrm{D}t} \\ & + \frac{1}{\sigma}\frac{\partial}{\partial y}\left(k\frac{\partial T}{\partial y}\right) + \frac{1}{\sigma}\frac{\partial}{\partial z}\left(k\frac{\partial T}{\partial z}\right),\end{aligned} \tag{2.7}$$

$$\gamma M^2 p = (1 + \alpha)\rho T. \tag{2.8}$$

Here we have used a mixed notation in which (v_1, v_2, v_3) is identified with (u, v, w) and (x_1, x_2, x_3) with (x, y, z). Repeated suffices β signify summation from 1 to 3. The functions λ, k, c_p and h denote in turn the bulk viscosity, the coefficient of heat conduction, the specific heat at constant pressure and the enthalpy per unit mass. The constants γ, M and σ are in turn the ratio of specific heats, the

Mach number and the Prandtl number defined by

$$\gamma = \frac{c_{p\infty}}{c_{v\infty}}, \quad M^2 = \frac{u_\infty^{*2}}{\gamma \bar{\Re} T_\infty^*} = \frac{u_\infty^{*2}}{a_\infty^2}, \quad \sigma = \frac{\mu_\infty c_{p\infty}}{k_\infty^*},$$

where $\bar{\Re}$ is a gas constant and $a_\infty = \sqrt{\gamma \bar{\Re} T_\infty^*}$ is the sound speed in the free stream. Finally, the function α in the equation of state (2.8) denotes the percentage by mass of the mixture which has been dissociated. Later in § 7 we shall give the expression for α for a specific dissociation model used in our discussion. In equations (2.4)–(2.7), the operator $\mathrm{D}/\mathrm{D}t$ is the material derivative and it has the usual expression appropriate to a rectangular coordinate system.

The basic state is given by

$$\left.\begin{aligned}(u, v, w) = (\bar{u}(x, y), \bar{v}(x, y), 0), \quad T = \bar{T}(x, y),\\ \rho = \bar{\rho}(x, y), \quad \mu = \bar{\mu}(x, y).\end{aligned}\right\} \tag{2.9}$$

By substituting (2.9) into the governing equations (2.3)–(2.8) it is straightforward to obtain the reduced equations satisfied by the basic state. The reader is referred to the book by Stewartson (1964) for a detailed discussion of these basic state equations. If we define the Howarth–Dorodnitsyn variable $\bar{y}$ and a similarity variable η by

$$\bar{y} = \int_0^y \bar{\rho}\, \mathrm{d}y \quad \text{and} \quad \eta = \frac{\bar{y}}{\sqrt{2x}}, \tag{2.10}$$

then the continuity equation is satisfied if $\bar{u}$ and $\bar{v}$ are written as

$$\bar{u} = f'(\eta), \quad \bar{v} = \frac{1}{\sqrt{2x}}\left[-\frac{1}{\bar{\rho}} f(\eta) + f'(\eta) \int_0^\eta \frac{1}{\bar{\rho}}\, \mathrm{d}\eta\right]. \tag{2.11}$$

Here the functions $f(\eta)$ and $\bar{T}(\eta)$ must satisfy

$$f f'' + (\bar{\rho}\bar{\mu} f'')' = 0, \tag{2.12}$$

$$\sigma^{-1}(\bar{\rho}\bar{k}\bar{T}')' + \bar{c}_p f \bar{T}' + \bar{\mu}(\gamma - 1) M^2 \bar{\rho} (f'')^2 = 0, \tag{2.13}$$

if the x-momentum and energy equations are to be satisfied. These equations must then be solved such that f, f' vanish at the wall, f', $\bar{T} = 1$ at infinity and either $\bar{T}' = 0$ or $\bar{T}$ specified at the wall. The y-momentum equation gives

$$\partial \bar{p}/\partial y = 0$$

to leading order so that $\bar{p} = \bar{p}(x)$. In our following analysis, we assume that there is no pressure gradient along the streamwise direction and therefore $\bar{p} = \text{const.} = 1/(\gamma M^2)$. Furthermore, it can be seen from (2.3)–(2.6) that the pressure perturbation should be of order $1/R$ and therefore equation (2.8) reduces to

$$[1 + \alpha(T)]\, \rho T = 1, \tag{2.14}$$

with the neglected term on the right-hand side being of order M^2/R. Note that in obtaining (2.12) and (2.13) we have not made any constitutive assumptions, so that they are valid for dissociated gases (to be discussed in § 7) as well as for undissociated ideal gases (to be discussed in §§ 3–6).

3. The strongly unstable inviscid mode

We first assume that the fluid is an ideal (one-component) gas undergoing no dissociation, so that $\alpha = 0$. Then we can assume that (i) the specific heats are constants; (ii) the coefficient of heat conduction is linearly related to the shear viscosity; and (iii) the enthalpy h is given by $h = c_p T$. These assumptions lead to the results

$$\bar{k} = \bar{\mu}, \quad \bar{c_p} = 1, \quad \bar{\rho} = \bar{T}^{-1}. \tag{3.1}$$

(Note that all of these quantities have been non-dimensionalized.) Then the basic equations (2.12) and (2.13) simplify to

$$f f'' + (\bar{\mu}\bar{T}^{-1} f'')' = 0, \tag{3.2}$$

$$\sigma^{-1}(\bar{\mu}\bar{T}^{-1}\bar{T}')' + f\bar{T}' + (\gamma - 1)M^2 \bar{\mu}\bar{T}^{-1}(f'')^2 = 0. \tag{3.3}$$

These two equations can then be solved if we make an constitutive assumption about the viscosity $\bar{\mu}$. In the previous paper, Hall & Fu (1989), we used Chapman's viscosity law. Here we use Sutherland's viscosity law, the dimensionless form of which is given by

$$\bar{\mu} = (1 + \tilde{m})\bar{T}^{3/2}/(\bar{T} + \tilde{m}), \tag{3.4}$$

where $\tilde{m}$ is a constant. Equation (3.4) is exact in the sense that it is derivable from the kinetic theories of gases (see Chapman & Cowling (1970) for a discussion of its validity, also compare (3.4) with (7.9)). At high Mach numbers we know from the work of for example Freeman & Lam (1959) that the basic state splits up into two distinct regions. Near the wall a boundary layer forms in which the downstream velocity approaches its free-stream value of unity while the temperature decreases from its value at the wall and ultimately decays algebraically at the edge of the layer. In the next region this algebraic decay is taken up and the temperature then approaches exponentially the free-stream value of unity. Here we shall refer to the layer near the wall as the inner region and the temperature adjustment layer as the outer region. It can be shown that the inner and outer regions are of thickness of order $M^{-1/2}$ and 1, respectively. Thus in the inner region, we define Y, $\tilde{T}$ and $F(Y)$ by

$$Y = M^{1/2}\eta, \quad \tilde{T} = M^{-2}\bar{T}, \quad F(Y) = M^{1/2} f. \tag{3.5}$$

Then equations (3.2) and (3.3) give

$$(1 + \tilde{m})\left(F''/\sqrt{\tilde{T}}\right)' + FF'' = 0, \tag{3.6}$$

$$\frac{1 + \tilde{m}}{\sigma}\left(\frac{\tilde{T}'}{\sqrt{\tilde{T}}}\right)' + F\tilde{T}' + (\gamma - 1)(1 + \tilde{m})\frac{(F'')^2}{\sqrt{\tilde{T}}} = 0 \tag{3.7}$$

to leading order. These equations are to be solved numerically subject to the conditions

$$\left.\begin{aligned} &F(0) = F'(0) = 0, \quad \tilde{T}(\infty) = 0, \quad F'(\infty) = 1, \\ &\tilde{T}'(0) = 0 \quad \text{if the wall is thermally insulated,} \\ &\tilde{T}(0) = n\tilde{T}_{\mathrm{w}} \quad \text{if the wall is under cooling,} \end{aligned}\right\} \tag{3.8}$$

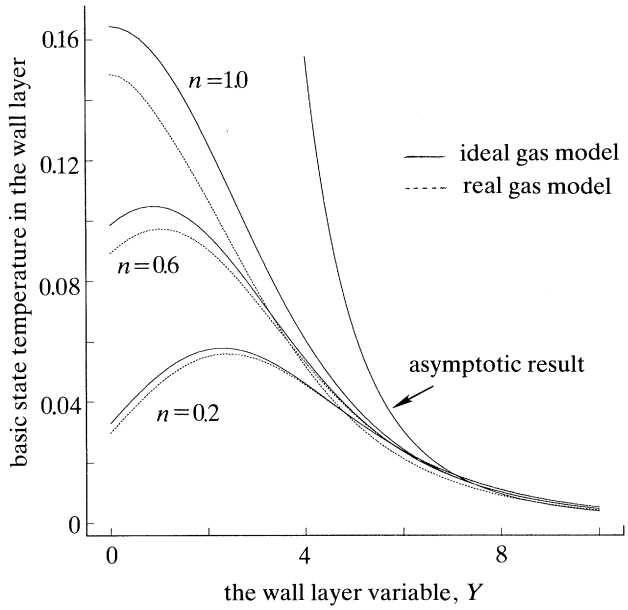

Figure 1. Basic state temperature in the wall layer for two models.

where $\tilde{T}_w$ is the wall temperature scaled on M^2T_∞ when the wall is thermally insulated and n is the wall cooling coefficient. Throughout this paper, we assume that $n = O(1)$. Thus the cooling we consider only modifies the basic state properties quantitatively and is mild compared with the severe cooling, considered by Seddougui *et al.* (1991) in the context of Tollmien–Schlichting wave instability, which drastically alters the basic state structure. The latter authors showed that severe wall cooling can have a significant destabilizing effect on Tollmien–Schlichting waves.

In figure 1 we have shown the results of our numerical integration of the wall layer equations (3.6) and (3.7). The temperature profiles are plotted for three values of the wall cooling coefficients: $n = 0.2$, 0.6 and 1.0 and were calculated with $\gamma = 1.4$, $\sigma = 0.72$, $\tilde{m} = 0.509$. The asymptotic profile for large Y given by equation (3.10) is also plotted there for comparison.

For large Y, equations (3.6) and (3.7) have the asymptotic solutions

$$F = Y - \beta + \frac{D}{(Y-\beta)^{3/\sigma}} + \cdots, \tag{3.9}$$

$$\tilde{T} = \frac{9(1+\tilde{m})^2}{\sigma^2}\frac{1}{(Y-\beta)^4} + \cdots, \tag{3.10}$$

where both β and D are to be determined by a numerical calculation. The numerical values of β corresponding to four values of the wall cooling coefficients are listed in table 1 together with the values of $F''(0)$, $\tilde{T}'(0)$ and $\tilde{T}(0)$.

The asymptotic expressions (3.9) and (3.10) imply that in the region $\eta = O(1)$, f and $\bar{T}$ expand as

$$f = \eta - \frac{\beta}{M^{1/2}} + \frac{\hat{f}(\eta)}{M^{3/2\sigma+1/2}}, \tag{3.11}$$

Table 1.

$n=$	0.2	0.4	0.6	0.8	1.0
$F''(0)$	0.151 7	0.199 7	0.231 7	0.256 0	0.2758
$\tilde{T}'(0)$	0.018 192	0.017 976	0.013 909	0.076 872	0
$\tilde{T}(0)$	0.032 86	0.065 72	0.098 58	0.131 44	0.1643
β	3.180 8	2.836 6	2.630 1	2.484 0	2.3721

$$\bar{T} = \hat{T}(\eta) + \cdots . \tag{3.12}$$

On substituting (3.11) and (3.12) into (3.2) and (3.3), we obtain to leading order

$$(1+\tilde{m})\left(\frac{\sqrt{\hat{T}}}{\hat{T}+\tilde{m}}\hat{f}''\right)' + \eta\hat{f}'' = 0, \tag{3.13}$$

$$\frac{(1+\tilde{m})}{\sigma}\left(\frac{\sqrt{\hat{T}}}{\hat{T}+\tilde{m}}\hat{T}'\right)' + \eta\hat{T}' = 0. \tag{3.14}$$

These two equations are to be solved numerically subject to the matching conditions

$$\text{as} \quad \eta \to 0, \quad \hat{f}(\eta) \sim \frac{D}{\eta^{3/\sigma}}, \quad \hat{T} \sim \frac{9(1+\tilde{m})^2}{\sigma^2}\frac{1}{\eta^4} + \cdots , \tag{3.15}$$

and the conditions at infinity

$$\hat{f}'(\infty) = 0, \quad \hat{T}(\infty) = 1. \tag{3.16}$$

The result from such a numerical calculation with $\tilde{m} = 0.509$ is shown in figure 2. In this figure the asymptotic result is the one given by (3.15).

It can be shown from (3.13) and (3.14) that

$$\hat{f}''(\eta) = \frac{D}{(1+\tilde{m})^{1+1/\sigma}}\left(\frac{\sigma}{12}\right)^{1/\sigma}\left(\frac{3}{\sigma}+1\right)\left(\frac{\hat{T}+\tilde{m}}{\sqrt{\hat{T}}}\right)^{1-1/\sigma}(-\hat{T}')^{1/\sigma}, \tag{3.17}$$

so that after (3.14) has been solved numerically, the function $\hat{f}''(\eta)$ can be computed easily from this equation. Also, we note that while the solution of (3.14) is independent of the inner region solution and thus of the conditions at the wall, the function $\hat{f}$ is dependent on the inner region solutions through the matching constant D.

We now assume, as in Hall & Fu (1989), that the flow is perturbed to a spanwise periodic stationary vortex structure with constant wavenumber a. The linearized stability equations for these Görtler vortices are then found by linearizing the Navier–Stokes equations (2.3)–(2.8) about the basic state and retaining the leading-order terms in the high Reynolds number limit. We obtain

$$\bar{T}^{-1}(\bar{u}U_x + \bar{v}U_y) + (\bar{\mu}a^2 + \bar{u}_x\bar{T}^{-1})U - (\bar{\mu}U_y)_y + \bar{T}^{-1}\bar{u}_y V - \{\bar{T}^{-2}(\bar{u}\bar{u}_x + \bar{v}\bar{u}_y) + (\tilde{\mu}\bar{u}_y)_y\}T - \tilde{\mu}\bar{u}_y T_y = 0, \tag{3.18}$$

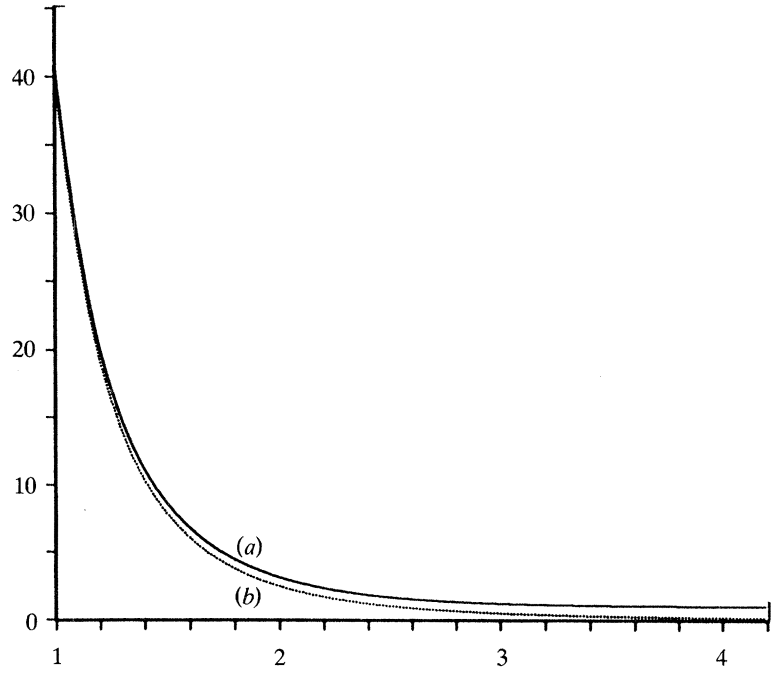

Figure 2. Basic state temperature in the adjustment layer. (*a*) Numerical calculation; (*b*) asymptotic result for small η.

$$\bar{T}^{-1}(\bar{v}_x + \kappa\bar{u}G)U + \tfrac{2}{3}\bar{\mu}_y U_x - \tfrac{1}{3}\bar{\mu}U_{xy} - \bar{\mu}_x U_y + \bar{T}^{-1}(\bar{u}V_x + \bar{v}V_y)$$
$$+ (\bar{\mu}a^2 + \bar{v}_y\bar{T}^{-1})V - \tfrac{4}{3}(\bar{\mu}V_y)_y + P_y$$
$$- [\bar{T}^{-2}(\bar{u}\bar{v}_x + \bar{v}\bar{v}_y + \tfrac{1}{2}\kappa G\bar{u}^2) + \tfrac{1}{3}\tilde{\mu}\bar{u}_{xy} - \tfrac{2}{3}\tilde{\mu}_y\bar{u}_x + \tfrac{4}{3}(\tilde{\mu}\bar{v}_y)_y + \tilde{\mu}_x\bar{u}_y]T$$
$$- \tilde{\mu}\bar{u}_y T_x - [-\tfrac{2}{3}\tilde{\mu}\bar{u}_x + \tfrac{4}{3}\tilde{\mu}\bar{v}_y]T_y + \tfrac{2}{3}\bar{\mu}_y \mathrm{i}aW - \tfrac{1}{3}\mathrm{i}a\bar{\mu}W_y = 0, \tag{3.19}$$

$$\bar{\mu}_x \mathrm{i}aU + \tfrac{1}{3}\bar{\mu}\mathrm{i}aU_x + \bar{\mu}_y \mathrm{i}aV + \tfrac{1}{3}\bar{\mu}\mathrm{i}aV_y - \mathrm{i}aP - \tfrac{2}{3}\tilde{\mu}(\bar{u}_x + \bar{v}_y)\mathrm{i}aT$$
$$- \bar{T}^{-1}(\bar{u}W_x + \bar{v}W_y) - \tfrac{4}{3}\mu a^2 W + (\bar{\mu}W_y)_y = 0, \tag{3.20}$$

$$2\bar{T}^{-3}(\bar{u}\bar{T}_x + \bar{v}\bar{T}_y)T - \bar{T}^{-2}(\bar{u}_x + \bar{v}_y)T - \bar{T}^{-2}(\bar{u}T_x + \bar{v}T_y)$$
$$+ \bar{T}^{-1}(U_x + V_y) - \bar{T}^{-2}(\bar{T}_x U + \bar{T}_y V) + \mathrm{i}a(W\bar{T}^{-1}) = 0, \tag{3.21}$$

$$\bar{T}^{-1}\bar{T}_x U - 2(\gamma-1)M^2\bar{\mu}\bar{u}_y U_y + \bar{T}^{-1}\bar{T}_y V + \bar{T}^{-1}(\bar{u}T_x + \bar{v}T_y) + (\bar{\mu}/\sigma)a^2 T$$
$$-\{\bar{T}^{-2}(\bar{u}\bar{T}_x + \bar{v}\bar{T}_y) + (\gamma-1)M^2\tilde{\mu}\bar{u}_y^2 + \sigma^{-1}(\tilde{\mu}\bar{T}_y)_y\}T$$
$$-\sigma^{-1}\tilde{\mu}\bar{T}_y T_y - \sigma^{-1}(\bar{\mu}T_y)_y = 0. \tag{3.22}$$

Here $\tilde{\mu} = \mathrm{d}\bar{\mu}/\mathrm{d}\bar{T}$, while (U, V, W), P and T denote the vortex velocity field, pressure and temperature, respectively. Equations (3.18)–(3.22) differ from equations (2.11 *a*–*e*) given in Hall & Fu (1989) only in that the bulk viscosity is taken to be zero here; that assumption is actually implied in that paper.

It was shown by Hall (1982) that in the incompressible case the neutral curve for small wavelength vortices has $G \sim a^4$ and that the vortices are confined to a layer of depth $a^{-1/2}$ where the flow is locally most unstable. Hall & Malik (1989)

extended this approach to the above system for $M = O(1)$ and wrote

$$G = g_0 a^4 + g_1 a^3 + \cdots .$$

They found that the leading-order growth rate $a^2\delta^*$ has δ^* given by

$$\delta^* = \frac{\bar{\mu}^2}{\sigma} + \left(\frac{\bar{u}^2 \bar{T}_y}{2\bar{T}^3} - \frac{\bar{u}\bar{u}_y}{\sigma \bar{T}^2} \right) g_0. \tag{3.23}$$

In the neutral case, $\delta^* = 0$ and (3.23) then determines the neutral Görtler number g_0 as a function of η. The most unstable location η^* is where g_0 has its minimum. In Hall & Fu (1989), it is found that when Chapman's law is used, η^* moves away from the wall as the Mach number increases. It is also found that the basic state temperature is $O(M^2)$ over most of the boundary layer and decreases rapidly to its free-stream value over a logarithmically thin adjustment layer sitting at the edge of the boundary layer. It is in this thin layer that η^* lies and hence where g_0 has its smallest order of magnitude in the large Mach number limit. Thus it is concluded that the thin temperature adjustment layer is most susceptible to Görtler vortices. From the preceding discussion in this section we see that when Sutherland's law is used, the logarithmically thin temperature adjustment layer corresponding to Chapman's law is now replaced by a more complex temperature adjustment layer of $O(1)$ thickness. If we still use (3.23) with $\delta^* = 0$ to calculate the orders of g_0 in the inner layer $\eta = O(M^{-1/2})$ and the outer temperature adjustment layer $\eta = O(1)$, we find that $g_0 = O(M^{15/2})$ in the former and $g_0 = O(1)$ in the latter. Hence once again the temperature adjustment layer is most susceptible to Görtler vortices with wavenumber of order one or larger. It should be noted, however, that the above conclusion is based upon a large wavenumber argument. In § 6 we show that the wall layer $\eta = O(M^{-1/2})$ is actually of order $M^{3/2}$ thickness in terms of the physical variable y. Thus Görtler vortices with wavelength comparable with the boundary layer thickness must be trapped in the wall layer and have $a = O(M^{-3/2})$. It is shown in § 6 that this wall mode has neutral Görtler number decreasing monotonically and has the centre of Görtler vortex activity moving towards the temperature adjustment layer as the wavenumber increases. Therefore, the minimum Görtler number corresponds to the mode trapped in the temperature adjustment layer and the latter is indeed the most dangerous mode when the whole range of wavenumbers are considered. It should also be noted that the result $g_0 = O(1)$ for the temperature adjustment layer is obtained by taking the large Mach number limit of the $O(1)$ Mach number and large wavenumber results. By doing so we have actually missed a term in the y-momentum equation related to the curvature of the basic state which is not important for the case $M = O(1)$ and $a \gg 1$, but is important in the large Mach number limit. As we show later on (see also Hall & Smith 1991), the curvature of the basic state produces an effective Görtler number of order $M^{3/2}$ in the absence of wall curvature so that instability can not occur for $g_0 = O(1)$.

(a) *The strongly unstable inviscid mode*

Let us first confine our attention to the mode trapped in the temperature adjustment layer. It is easy to show with the aid of expressions (3.11) and (3.12)

that in this temperature adjustment layer,

$$\bar{u}\bar{v}_x + \bar{v}\bar{v}_y = -(2x)^{-3/2}[BM^{3/2} + \bar{\mu}\bar{T}'/\sigma\bar{T} - \eta^2\bar{T}'] + o(1), \tag{3.24}$$

where

$$B \overset{\text{def}}{=} \lim_{M\to\infty} M^{-3/2} \int_0^\infty \bar{T}(\eta)\,\mathrm{d}\eta. \tag{3.25}$$

The first term on the right-hand side of (3.24) is the term the importance of which has been mentioned earlier. An investigation of the y-momentum equation (3.19) shows that the Görtler number must be of order $M^{3/2}$ to enter the leading-order analysis. Thus we write

$$\tfrac{1}{2}\kappa(x)G = G^*(x)M^{3/2}, \tag{3.26}$$

so that for a given constant Görtler number G we compute $G^*(x)$ by using

$$G^*(x) = \tfrac{1}{2}\kappa(x)GM^{-3/2}. \tag{3.27}$$

For convenience, we also define another function $Q(x)$ by

$$Q(x) = B(2x)^{-3/2}, \tag{3.28}$$

so that

$$\bar{u}\bar{v}_x + \bar{v}\bar{v}_y + \tfrac{1}{2}\kappa(x)G\bar{u}^2 = (G^* - Q)M^{3/2} + o(M^{3/2}). \tag{3.29}$$

With the use of this relation, we can deduce from the perturbation equations (3.18)–(3.22) that

$$V = O(M^{3/4}T), \quad W = O(M^{3/4}T), \quad P = O(M^{3/2}T), \quad U = O(M_1^{-1}T), \tag{3.30}$$

and that for fixed η,

$$\partial/\partial x = O(M^{3/4}),$$

where $M_1 \overset{\text{def}}{=} 1/M^{3/2\sigma+1/2}$. We therefore look for asymptotic solutions of the form

$$\left.\begin{aligned}
T &= \exp\left(M^{3/4}\int^x \beta(x)\,\mathrm{d}x\right)\{T_0(x,\eta) + M^{-3/4}T_1(x,\eta) + \cdots\},\\
U &= M_1^{-1}\exp\left(M^{3/4}\int^x \beta(x)\,\mathrm{d}x\right)\{U_0(x,\eta) + M^{-3/4}U_1(x,\eta) + \cdots\},\\
V &= M^{3/4}\exp\left(M^{3/4}\int^x \beta(x)\,\mathrm{d}x\right)\{V_0(x,\eta) + M^{-3/4}V_1(x,\eta) + \cdots\},\\
W &= M^{3/4}\exp\left(M^{3/4}\int^x \beta(x)\,\mathrm{d}x\right)\{W_0(x,\eta) + M^{-3/4}W_1(x,\eta) + \cdots\},\\
P &= M^{3/2}\exp\left(M^{3/4}\int^x \beta(x)\,\mathrm{d}x\right)\{P_0(x,\eta) + M^{-3/4}P_1(x,\eta) + \cdots\},
\end{aligned}\right\} \tag{3.31}$$

where the spatial amplification has been taken care of by using the WKB method and $\beta(x)$ is the local growth rate to be determined. On substituting (3.31) into (3.18)–(3.22) and then equating the coefficients of like powers of M, we obtain a hierarchy of equations. To leading order, we find that V_0 satisfies the differential

equation

$$\frac{\partial^2 V_0}{\partial \eta^2} - \frac{2\bar{T}'}{\bar{T}}\frac{\partial V_0}{\partial \eta} - \tilde{k}^2 \bar{T}^2 V_0 = \frac{\tilde{k}^2}{\sqrt{2x}\,\beta^2}(G^* - Q)\bar{T}' V_0, \tag{3.32}$$

while T_0, W_0 and P_0 are related to V_0 by

$$T_0 = -\frac{\bar{T}'}{\sqrt{2x}\,\bar{T}\beta}V_0, \quad \mathrm{i}aW_0 = -\frac{1}{\sqrt{2x}\,\bar{T}}\frac{\partial V_0}{\partial \eta}, \quad P_0 = -\frac{\beta\sqrt{2x}}{\bar{T}^2\tilde{k}^2}\frac{\partial V_0}{\partial \eta}, \tag{3.33}$$

and U_0 does not appear in our leading-order analysis. Here $\tilde{k} \overset{\text{def}}{=} \sqrt{2x}\,a$ is the local wavenumber. Equation (3.32) subject to V_0 vanishing at $\eta = 0, \infty$ is a Sturm–Liouville problem which has solutions if

$$(G^* - Q)\bar{T}'/\beta^2 \leq 0.$$

This means that

$$\beta^2 \geq 0 \quad \text{if} \quad G^* \geq Q, \qquad \beta^2 \leq 0 \quad \text{if} \quad G^* \leq Q,$$

since $\bar{T}' < 0$. It then follows that neutral stability ($\beta = 0$) occurs at the position $x = x_n$ where

$$G^*(x_n) = Q(x_n) \tag{3.34}$$

at zero order. Therefore, in view of the definitions (3.27) and (3.28), the neutral Görtler number has the expansion

$$G = \frac{2B}{\kappa(x_n)(2x_n)^{3/2}}M^{3/2} + \text{higher-order correction terms.} \tag{3.35}$$

On comparing this expression with Hall & Fu's (1989) equation (3.7), which is valid for Chapman's law fluids and in which the first term on the right-hand side is of order M^2, we can immediately conclude that using Chapman's viscosity law predicts a larger Görtler number than using Sutherland's viscosity law.

For the rest of this paper we shall take G_N to be the zero-order approximation to the *critical inviscid Görtler number*, thus G_N is obtained by retaining only the first term on the right-hand side of (3.35). An important point concerning (3.35) is that the first term on the right-hand side is independent of x_n if the wall curvature varies like $x^{-3/2}$; in the latter situation non-parallel effects dominate and the vortex growth rate is smaller. Thus to determine the higher-order correction terms to the neutral Görtler number, we have to distinguish two cases: (i) $\kappa(x) = (2x)^{-3/2}$ and (ii) $\kappa(x) \neq (2x)^{-3/2}$. They will be treated separately in the next two sections.

On the other hand, equation (3.32) can also be interpreted as an eigenvalue problem which determines the growth rate $\beta(x)$ at a given value of x corresponding to any wavenumber $\tilde{k}$. The appropriate boundary conditions are deduced as follows. As $\eta \to \infty$, $\bar{T} \to 1$ and equation (3.32) reduces to

$$\frac{\partial^2 V_0}{\partial \eta^2} - \tilde{k}^2 V_0 = 0,$$

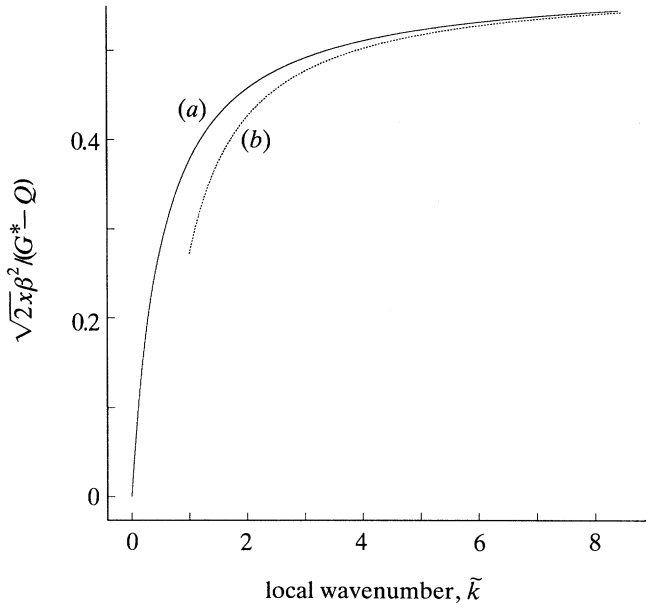

Figure 3. The dependence of the eigenvalue $\sqrt{2x}\beta^2/(G^* - Q)$ of (3.32) on the local wavenumber $\tilde{k}$, which agrees with the results from asymptotic analysis that as $\tilde{k} \to 0$, $\sqrt{2x}\beta^2/(G^* - Q)$ is of order $\tilde{k}$; while as $\tilde{k} \to \infty$, $\sqrt{2x}\beta^2/(G^* - Q)$ tends to the constant 0.5786. (*a*) Numerical result; (*b*) asymptotic result.

so that $V_0 \sim \exp(-\tilde{k}\eta)$ and the asymptotic condition

$$\frac{\partial V_0}{\partial \eta} + \tilde{k} V_0 = 0 \tag{3.36}$$

should be imposed at 'infinity'. As $\eta \to 0$, $\bar{T} \to A^2/\eta^4$ where from (3.15*b*) $A = 3(1 + \tilde{m})/\sigma$. Equation (3.32) reduces to

$$\frac{\partial^2 V_0}{\partial \eta^2} + \frac{8}{\eta}\frac{\partial V_0}{\partial \eta} - \frac{\tilde{k}^2 A^4}{\eta^8} V_0 = -\frac{(G^* - Q)\tilde{k}^2}{\sqrt{2x}\,\beta^2} \cdot \frac{4A^2}{\eta^5} V_0, \tag{3.37}$$

which has the solution

$$V_0 \sim \exp(-\tilde{k}A^2/3\eta^3). \tag{3.38}$$

Hence the asymptotic condition

$$\frac{\partial V_0}{\partial \eta} - \frac{\tilde{k}A^2}{\eta^4} V_0 = 0 \tag{3.39}$$

should be imposed at 'zero' (which is taken to be some small value in numerical calculation).

The eigenvalue problem (3.32), (3.36) and (3.39) was solved numerically by using a fourth-order Runge–Kutta method. In figure 3, we have shown the de-

pendence of the growth rate on the local wavenumber. The plot clearly shows that as $\tilde{k} \to 0$, $\beta^2 \to 0$ while as $\tilde{k} \to \infty$, $\beta^2 \to$ const. These features are also borne out by the asymptotic analysis given in the following subsection. The inviscid mode we have described above therefore has growth rate proportional to $M^{3/4}$ and we refer to it as the *strongly unstable inviscid mode*. We note that when $G^* = Q$ the growth rate vanishes. In this case it is necessary to look for evolution of the vortices on a shorter lengthscale in the streamwise direction; that problem will be addressed later in this paper and we shall refer to the inviscid mode in that régime as the *near neutral inviscid mode*.

(*b*) *The small and large wavenumber limits of the strongly unstable inviscid mode*

First, we note that as $\tilde{k} \to 0$, we are approaching the scalings for the wall mode (see § 6) which has wavenumber $\tilde{k} \sim O(M^{-3/2})$ and which is trapped in the wall layer. Thus Görtler vortices are appropriately governed by (3.37). The solution (3.38) shows that vortices decay to zero in the thin layer $\eta = O(\tilde{k}^{1/3})$ near the wall. This is also verified by the obvious shift to the left of the first mode eigenfunctions in figure 4 with decreasing $\tilde{k}$. It can then be deduced from (3.37) that β^2 has to be $O(\tilde{k})$ to enter the leading-order analysis.

Next, in the large $\tilde{k}$ limit, a WKB analysis of (3.32) shows that Görtler vortices will be trapped in an $O(\tilde{k}^{-1/2})$ thin layer centred at $\eta = \eta^*$ where β^2 has a maximum. Thus we introduce a new variable ζ by

$$\zeta = \tilde{k}^{1/2}(\eta - \eta^*), \tag{3.40}$$

expand $(G^* - Q)/(\sqrt{2x}\,\beta^2)$ as

$$\frac{G^* - Q}{\sqrt{2x}\,\beta^2} = \lambda_0 + \tilde{k}^{-1/2}\lambda_1 + \tilde{k}^{-1}\lambda_2 + \cdots, \tag{3.41}$$

and look for solutions of the form

$$V_0(x, \eta) = V_0^0(x, \zeta) + \tilde{k}^{-1/2}V_0^1(x, \zeta) + \tilde{k}^{-1}V_0^2(x, \zeta) + \cdots. \tag{3.42}$$

On substituting (3.40)–(3.42) into (3.32), equating the coefficients of like powers of $\tilde{k}$, and then solving the resulting set of equations, we find that to leading order, λ_0 is determined as

$$\lambda_0 = -\bar{T}^2(\eta^*)/\bar{T}'(\eta^*). \tag{3.43}$$

At order $\tilde{k}^{-1/2}$, λ_1 is determined as $\lambda_1 = 0$ if we insist that β^2 attains its maximum at $\eta = \eta^*$. At order $\tilde{k}^{-1}$, V_0^0 is found to satisfy the parabolic-cylinder equation

$$\frac{\partial^2 V_0^0}{\partial \xi^2} - \tfrac{1}{4}\xi^2 V_0^0 - aV_0^0 = 0, \tag{3.44}$$

where

PHILOSOPHICAL TRANSACTIONS OF THE ROYAL SOCIETY A MATHEMATICAL, PHYSICAL & ENGINEERING SCIENCES

$$\left.\begin{aligned}\xi &= \sqrt{2}\,\bar{T}(\eta^*)\left\{\frac{1}{2\bar{T}'(\eta^*)}\frac{\mathrm{d}^2}{\mathrm{d}\eta^{*2}}\left(\frac{1}{\lambda_0}\right)\right\}^{1/4}\zeta,\\ \bar{a} &= \frac{\lambda_2\bar{T}'(\eta^*)}{2\bar{T}^2(\eta^*)}\left\{\frac{1}{2\bar{T}'(\eta^*)}\frac{\mathrm{d}^2}{\mathrm{d}\eta^{*2}}\left(\frac{1}{\lambda_0}\right)\right\}^{-1/2}.\end{aligned}\right\} \tag{3.45}$$

If we impose the condition that the disturbance is confined to the $\tilde{k}^{-1/2}$ layer we must choose $\bar{a} = -\frac{1}{2} - s$, where s is a non-negative integer. This condition determines the infinite sequence of eigenvalues

$$\lambda_2 = \lambda_{2s} = \lambda_0\frac{1+2s}{\sqrt{-2\bar{T}'(\eta^*)}}\sqrt{-\frac{\mathrm{d}^2}{\mathrm{d}\eta^{*2}}\left(\frac{1}{\lambda_0}\right)}. \tag{3.46}$$

The eigenfunctions corresponding to the eigenvalue λ_{2s} are given by

$$V_0^0 = V_{0s}^0 = \mathrm{e}^{-\frac{1}{4}\xi^2}He_s(\xi), \tag{3.47}$$

where $He_s(\xi)$ is a Hermite polynomial.

With the aid of the numerical values for $\bar{T}$ given earlier in this section, we find that

$$\frac{\sqrt{2x}\,\beta^2}{G^* - Q} = 0.5786\left\{1 - 0.5297\frac{1+2s}{\tilde{k}} + \cdots\right\}, \tag{3.48}$$

and that $\eta^* = 2.3228$. Both these numerical values and the concentration of vortices in an $O(\tilde{k}^{-1/2})$ region are confirmed by the numerical results shown in figures 3 and 5.

In closing this section, we note that results given here for hypersonic flows are in sharp contrast with related results for incompressible flows. In a recent paper, Denier *et al.* (1990) have discussed the spectrum of the large Görtler number eigenvalue problem. It was found that the inviscid Görtler vortex eigenvalue problem has an exact solution with the spatial growth rate increasing monotonically from zero and tending to infinity at large wavenumbers. In the high wavenumber limit viscous effects become important when the wavenumber is $O(G^{1/5})$ and a maximum growth rate is achieved in that régime with the growth rate tending to zero in an $O(G^{1/4})$ régime as discussed by Hall (1982). At small wavenumbers the growth rate tends to zero and the vortices spread out above the boundary layer. In fact when the wavenumber is $O(G^{-1/7})$ an eigenvalue problem related to that for Tollmien–Schlichting waves is recovered but at even smaller wavenumbers non-parallel effects dominate and the problem must be solved numerically as in Hall (1983). The major difference we have found above for hypersonic Görtler vortices is that the growth rate tends to a finite value as the local wavenumber tends to infinity; we shall see later that this has a significant effect on the way in which viscous effects come into play at high wavenumbers.

4. Neutral instability with $\kappa(x) \sim (2x)^{-3/2}$

We now proceed with the determination of the higher-order correction terms in the neutral Görtler number expansion (3.35). In the case when the curvature

Figure 4

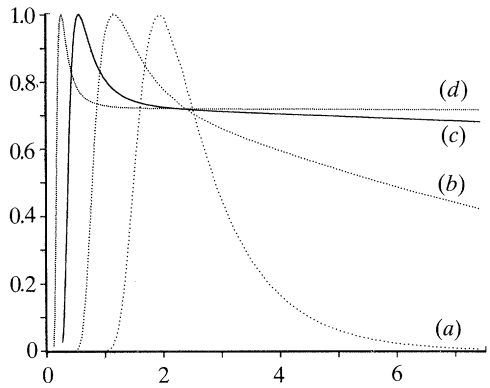

Figure 5

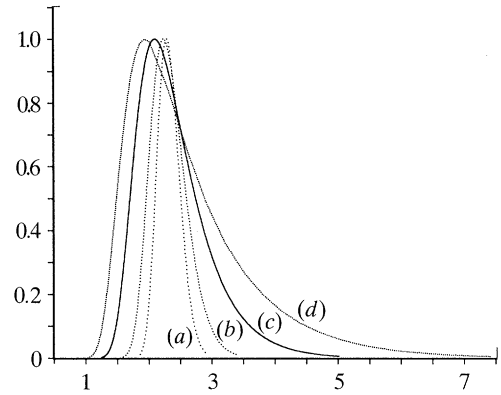

Figure 4. The eigenfunctions of (3.32) corresponding to a set of decreasing wavenumbers $\tilde{k}$. Asymptotic analysis shows that as $\tilde{k} \to 0$, vortices are confined to a wall layer of $O(\tilde{k}^{1/3})$ thickness and V_0 tends to a constant when moving away from the wall layer. (*a*) $k = 1$; (*b*) $k = 0.1$; (*c*) k=0.01;(d)$k = 0.001$.

Figure 5. The eigenfunctions of (3.32) corresponding to a set of increasing wavenumbers $\tilde{k}$. Asymptotic analysis shows that as $\tilde{k} \to \infty$, vortices are confined to an $O(\tilde{k}^{-1/2})$ thin layer centred at $\eta = 2.3228$, where $-\bar{T}'/\bar{T}^2$ attains its maximum. (*a*) $k = 15$; (*b*) $k = 6$; (*c*) $k = 2$; (*d*) $k = 1$.

$\kappa(x) = (2x)^{-3/2}$, $G^*(x) = Q(x)$ and the $O(M^{3/2})$ term on the right-hand side of (3.29) vanishes for all x. The implication of this is that for this special distribution the curvature of the basic state is exactly counteracted by wall curvature over an $O(1)$ interval in x, in the more general case that is only the case over an asymptotically small interval. An investigation of the perturbation equations (3.18)–(3.22) with the aid of the equations (A 1)–(A 5) given in Appendix A then reveals that the neutral Görtler number must expand as

$$G = 2BM^{3/2} + \tilde{G} + o(1), \tag{4.1}$$

and that the perturbation quantities have relative orders

$$U = O(M_1^{-1}V), \quad T = O(V), \quad W = O(V), \quad P = O(V),$$

where $\tilde{G} = O(M^0)$ is to be determined. We therefore look for the following form of solutions for (3.18)–(3.22):

$$\left.\begin{aligned} U = M_1^{-1}\tilde{U}(x,\eta) + \cdots, \quad V = \tilde{V}(x,\eta) + \cdots, \quad W = \tilde{W}(x,\eta) + \cdots, \\ P = (\sqrt{2x})^{-1/2}\tilde{P}(x,\eta) + \cdots, \quad T = \sqrt{2x}\,\tilde{\theta}(x,\eta) + \cdots, \end{aligned}\right\} \tag{4.2}$$

where the insertion of the factor $\sqrt{2x}$ is purely for convenience.

On substituting (4.2) into (3.18)–(3.22) and then equating the coefficients of

like powers of M, we obtain, to leading order,

$$\frac{\partial}{\partial\eta}\left(\frac{\bar{\mu}}{\bar{T}}\frac{\partial\tilde{U}}{\partial\eta}\right)+\eta\frac{\partial\tilde{U}}{\partial\eta}-\bar{\mu}\bar{T}\tilde{k}^2\tilde{U}-2x\frac{\partial\tilde{U}}{\partial x}$$
$$=\sqrt{2x}\left\{\frac{\hat{f}''}{\bar{T}}\tilde{V}+\left[\frac{\eta}{\bar{T}}\hat{f}''-\frac{\partial}{\partial\eta}\left(\frac{\tilde{\mu}\hat{f}''}{\bar{T}}\right)\right]\tilde{\theta}-\frac{\tilde{\mu}\hat{f}''}{\bar{T}}\frac{\partial\tilde{\theta}}{\partial\eta}\right\}, \tag{4.3}$$

$$\frac{\partial\tilde{P}}{\partial\eta}=\frac{\eta\bar{T}'}{\bar{T}}\tilde{V}+\eta\frac{\partial\tilde{V}}{\partial\eta}-\bar{\mu}\tilde{k}^2\bar{T}\tilde{V}+\tfrac{4}{3}\frac{\partial}{\partial\eta}\left(\frac{\bar{\mu}}{\bar{T}}\frac{\partial\tilde{V}}{\partial\eta}\right)$$
$$+\frac{\tilde{\theta}}{\bar{T}}\left[\eta^2\bar{T}'-\frac{\bar{\mu}\bar{T}'}{\sigma\bar{T}}+\tfrac{1}{2}\tilde{G}-\tfrac{4}{3}\bar{T}\frac{\partial}{\partial\eta}\left(\frac{\tilde{\mu}\eta\bar{T}'}{\bar{T}}\right)\right]$$
$$-\frac{4}{3\bar{T}}\tilde{\mu}\eta\bar{T}'\frac{\partial\tilde{\theta}}{\partial\eta}-\tfrac{2}{3}\tilde{\mu}\bar{T}'\mathrm{i}\tilde{k}\tilde{W}+\tfrac{1}{3}\bar{\mu}\frac{\partial}{\partial\eta}(\mathrm{i}\tilde{k}\tilde{W})-2x\frac{\partial\tilde{V}}{\partial x}, \tag{4.4}$$

$$\frac{\partial}{\partial\eta}\left(\frac{\bar{\mu}}{\bar{T}}\frac{\partial\tilde{W}}{\partial\eta}\right)=-\tilde{\mu}\bar{T}'\mathrm{i}\tilde{k}\tilde{V}-\tfrac{1}{3}\bar{\mu}\mathrm{i}\tilde{k}\frac{\partial\tilde{V}}{\partial\eta}+\mathrm{i}\tilde{k}\bar{T}\tilde{P}$$
$$-\tfrac{2}{3}\tilde{\mu}\eta\bar{T}'\mathrm{i}\tilde{k}\tilde{\theta}-\eta\frac{\partial\tilde{W}}{\partial\eta}+\tfrac{4}{3}\bar{\mu}\tilde{k}^2\bar{T}\tilde{W}+2x\frac{\partial\tilde{W}}{\partial x}, \tag{4.5}$$

$$\frac{\partial}{\partial\eta}\left(\frac{\tilde{V}}{\bar{T}}\right)+\frac{\eta}{\bar{T}}\frac{\partial\tilde{\theta}}{\partial\eta}=-\mathrm{i}\tilde{k}\tilde{W}+\left(1+\frac{\eta\bar{T}'}{\bar{T}}\right)\frac{\tilde{\theta}}{\bar{T}}+\frac{2x}{\bar{T}}\frac{\partial\tilde{\theta}}{\partial x}, \tag{4.6}$$

$$\frac{1}{\sigma}\frac{\partial}{\partial\eta}\left(\frac{\bar{\mu}}{\bar{T}}\frac{\partial\tilde{\theta}}{\partial\eta}\right)=-\left(\eta+\frac{\tilde{\mu}\bar{T}'}{\sigma\bar{T}}\right)\frac{\partial\tilde{\theta}}{\partial\eta}+\frac{\bar{T}'}{\bar{T}}\tilde{V}$$
$$+\tilde{\theta}\left[1+\frac{\eta\bar{T}'}{\bar{T}}-\frac{1}{\sigma}\frac{\partial}{\partial\eta}\left(\frac{\tilde{\mu}\bar{T}'}{\bar{T}}\right)+\frac{\mu}{\sigma}\bar{T}\tilde{k}^2\right]+2x\frac{\partial\tilde{\theta}}{\partial x}. \tag{4.7}$$

Here $\tilde{k}\overset{\text{def}}{=}\sqrt{2x}\,a$. It can be seen that (4.4)–(4.7) are independent of $\tilde{U}$ and the latter is determined from (4.3) after $(\tilde{V},\tilde{W},\tilde{T},\tilde{P})$ have been determined. Since these leading-order perturbation equations are parabolic with respect to the variable x, they have to be solved by specifying the perturbation quantities at a given upstream position and then marching downstream. We therefore expect that neutral stability would depend crucially on what initial conditions we impose and where we impose them. However, before we present our numerical solutions of these equations, we first consider a special case: the large wavenumber limit for which a simple asymptotic solution is possible.

(*a*) *Large wavenumber limit*

In the large wavenumber limit, the lengthscale over which vortices vary is small compared with the lengthscale over which the boundary layer grows. Then we expect that non-parallel effects do not come into our leading-order analysis. This is indeed the case, as we show below.

For large $\tilde{k}$, vortices are confined to a thin layer of $O(\epsilon^{1/2})$ thickness centred

on $\eta = \eta^*$, where

$$\epsilon \stackrel{\text{def}}{=} 1/\tilde{k}, \tag{4.8}$$

and where η^* is the most unstable position to be determined in the course of our calculation. We therefore define a new variable ϕ by

$$\phi = \epsilon^{-1/2}(\eta - \eta^*).$$

An investigation of equations (4.3)–(4.7) shows that when $\epsilon \to 0$,

$$\left.\begin{gathered} \tilde{\theta} = O(\epsilon^2 \tilde{V}), \quad \tilde{W} = O(\epsilon^{1/2}\tilde{V}), \quad \tilde{P} = O(\epsilon^{-1/2}\tilde{V}), \\ \tilde{G} = O(1/\epsilon^4), \quad \partial/\partial x = O(1/\epsilon^2). \end{gathered}\right\} \tag{4.9}$$

Hence we look for the following form of asymptotic solutions for (4.3)–(4.7):

$$\left.\begin{gathered} \tilde{G} = \epsilon^{-4}(G_0 + \epsilon^{1/2}G_1 + \epsilon G_2 + \epsilon^{3/2}G_3 + \cdots), \\ \tilde{V} = (V_0 + \epsilon^{1/2}V_1 + \cdots)E, \quad \tilde{W} = (\epsilon^{1/2}W_0 + \epsilon W_1 + \cdots)E, \\ \tilde{P} = (\epsilon^{-1/2}P_0 + P_1 + \cdots), \quad \tilde{\theta} = (\epsilon^2\theta_0 + \epsilon^{5/2}\theta_1 + \cdots)E, \end{gathered}\right\} \tag{4.10}$$

where

$$E = \exp\left\{\frac{1}{\epsilon^2}\int^x (\beta_0(\phi) + \epsilon^{1/2}\beta_1(\phi) + \cdots)\,\mathrm{d}\phi\right\}, \tag{4.11}$$

and where V_0, V_1, etc., are functions of ϕ and x. Note that E here represents the fast variation of the perturbation quantities along the streamwise direction while the dependence of V_0, W_0, etc., on x represent the slow variation of perturbation quantities due to the non-parallel effect of the boundary layer growth. In effect we have described the fast variation of the disturbance by a WKB type of expansion in the streamwise direction. Here we are only concerned with neutral stability, so we set $\beta_0 = \beta_1 = \beta_2 = 0$. On substituting (4.10) into (4.3)–(4.7) and then equating the coefficients of like powers of ϵ, we obtain a hierarchy of matrix equations. To leading order, we have

$$\theta_0 = -\frac{\sigma\bar{T}_1}{\bar{\mu}_0\bar{T}_0^2}V_0, \quad \mathrm{i}W_0 = -\frac{1}{\bar{T}_0}\frac{\partial V_0}{\partial\phi}, \quad P_0 = -\frac{\bar{\mu}_0}{\bar{T}_0}\frac{\partial V_0}{\partial\phi}, \quad G_0 = -\frac{2\bar{\mu}_0^2\bar{T}_0^4}{\sigma\bar{T}_1}, \tag{4.12}$$

where $\bar{T}_0 = \bar{T}(\eta^*)$, $\bar{T}_1 = \bar{T}'(\eta^*)$ and $\bar{\mu}_0 = \bar{\mu}(\bar{T}_0)$. To next order, we deduce that

$$G_1 = 0. \tag{4.13}$$

At next order we find that V_0 must satisfy the parabolic-cylinder equation

$$\frac{\partial^2 V_0}{\partial\zeta^2} - \tfrac{1}{4}\zeta^2 V_0 - \hat{a}V_0 = 0. \tag{4.14}$$

Here

$$\zeta = \phi\lambda^{1/4}, \quad \hat{a} = G_2\frac{\sigma\bar{T}_0'}{6\bar{\mu}_0^2\bar{T}_0^2}\lambda^{-1/2}, \quad \lambda = -\frac{2\bar{T}_0^2}{3G_0}\left(\frac{\partial^2 G_0}{\partial\eta^2}\right)_{\eta=\eta^*}. \tag{4.15}$$

If we impose the condition that the disturbance is confined to the $\epsilon^{1/2}$ layer we must choose

$$\hat{a} = -\tfrac{1}{2} - s, \quad s = 0, 1, \ldots. \tag{4.16}$$

The smallest G_2 corresponds to $s = 0$ and we then have from (4.15 *b*) that

$$G_2 = \left(\frac{3G_0}{2\bar{T}_0^2} \frac{\partial^2 G_0}{\partial \eta^2} \right)^{1/2}_{\eta=\eta^*}. \tag{4.17}$$

The centre of vortex activity η^* is determined by the condition that G_0 attains its minimum there:

$$\left(\frac{\partial G_0}{\partial \eta} \right)_{\eta=\eta^*} = 0. \tag{4.18}$$

After solving (3.14) numerically for the basic state temperature $\bar{T}$, we then use (4.12 *d*) and (4.18) to determine η^*, and (4.12 *d*) and (4.17) to determine G_0 and G_2. We find that

$$\eta^* = 3.001, \quad G_0 = 15.4834, \quad G_2 = 34.3175,$$

so that

$$\tilde{G} = 15.4834\tilde{k}^4 + 34.3175\tilde{k}^3 + \cdots. \tag{4.19}$$

Finally, we remark that the above analysis is valid as long as the local wavenumber $\tilde{k} = \sqrt{2x}\, a$ is large. This means that the far downstream evolution of Görtler vortices can always be described by the above theory.

(*b*) *Numerical results for* $\tilde{k} \sim O(1)$

When the wavenumber is $O(1)$, the perturbation equations (4.3)–(4.7) are parabolic with respect to x and they have to be solved numerically subject to some initial conditions imposed at some upstream position $\bar{x}$. For computational purpose it is convenient to eliminate $\tilde{P}$ and $\tilde{W}$ among (4.4)–(4.5). After some manipulation, we obtain

$$-\frac{1}{\bar{T}} \frac{\partial^4 \tilde{V}}{\partial \eta^4} + \frac{2x}{\bar{\mu}} \frac{\partial^3 \tilde{V}}{\partial x \partial \eta^2} - \frac{4x\bar{T}'}{\bar{\mu}\bar{T}} \frac{\partial^2 \tilde{V}}{\partial x \partial \eta} - \frac{\tilde{k}^2 \bar{T}^2}{\bar{\mu}} 2x \frac{\partial \tilde{V}}{\partial x} = \sum_{i=1}^{9} a_i, \tag{4.20}$$

$$\frac{\bar{\mu}}{\sigma\bar{T}} \frac{\partial^2 \tilde{\theta}}{\partial \eta^2} = \left(\frac{\bar{\mu}\bar{T}'}{\sigma\bar{T}^2} - \frac{2\tilde{\mu}\bar{T}'}{\sigma\bar{T}} - \eta \right) \frac{\partial \tilde{\theta}}{\partial \eta} + \frac{\bar{T}'}{\bar{T}} \tilde{V} + 2x \frac{\partial \tilde{\theta}}{\partial x} + \left[1 + \frac{\eta\bar{T}'}{\bar{T}} - \frac{1}{\sigma} \frac{\partial}{\partial \eta} \left(\frac{\tilde{\mu}\bar{T}'}{\bar{T}} \right) + \frac{\bar{\mu}}{\sigma} \bar{T}\tilde{k}^2 \right] \tilde{\theta}, \tag{4.21}$$

where the expressions for a_i are given in Appendix B to this paper. The finite difference scheme used here is similar to that used by Hall (1983), Wadey (1993) for incompressible flows. The reader is referred to the latter papers for a more detailed discussion. Our implementation of the numerical scheme is as follows. We first specify $\tilde{V}$, $\tilde{U}$ and $\tilde{\theta}$ at a given upstream position $\bar{x}$. Then we use the finite difference scheme to march downstream and thus calculate the evolution of the initial perturbation with respect to the streamwise variable x. The position of neutral stability is defined as the place where a certain energy measure has zero growth rate. We use the following five energy measures to monitor the energy

variation:

$$E_1 = \int_0^\infty \tilde{U}^2 \,\mathrm{d}y = \sqrt{2x} \int_0^\infty \tilde{U}^2 \bar{T} \,\mathrm{d}\eta, \tag{4.22}$$

$$E_2 = \int_0^\infty (\tilde{V}^2 + \tilde{W}^2) \,\mathrm{d}y = \sqrt{2x} \int_0^\infty (\tilde{V}^2 + \tilde{W}^2) \bar{T} \,\mathrm{d}\eta, \tag{4.23}$$

$$E_3 = \int_0^\infty \sqrt{2x}\, \tilde{\theta} \,\mathrm{d}y = 2x \int_0^\infty \tilde{\theta} \bar{T} \,\mathrm{d}\eta, \quad E_4 = \tilde{U}_{\max}, \tag{4.24}$$

$$E_5 = \int_0^\infty \left(\frac{\partial \tilde{U}}{\partial y} \right)^2 \mathrm{d}y = \frac{1}{\sqrt{2x}} \int_0^\infty \frac{1}{\bar{T}} \left(\frac{\partial \tilde{U}}{\partial \eta} \right)^2 \mathrm{d}\eta. \tag{4.25}$$

We give results for several measures of the vortex strength to show the relatively large variation of growth rates associated with different flow quantities. Depending on the initial conditions and on which energy measure we use, the disturbance can either grow or decay initially. In the former case, there is only one neutral position corresponding to each pair $(\tilde{k}, \tilde{G})$: the energy will reach a maximum at some downstream location and then decay to zero monotonically. The corresponding neutral curves only have right branches. The region on the left of a neutral curve is unstable and the region on the right is stable. In the latter case, if the Görtler number is large enough, there are always two neutral positions: the energy will reach a minimum at some downstream location, then grow to reach a maximum and finally decay to zero monotonically. The corresponding neutral curves have distinct right and left branches. The region above a neutral curve is unstable and other regions are stable. For the special curvature case discussed in the present section, the flow is always stable for $x \gg 1$, since according to the asymptotic result obtained in the previous subsection, the flow is neutrally stable where $\tilde{G} \sim \tilde{k}^4$ for $\tilde{k} \gg 1$ so that $\kappa(x)$ must increase at least as quickly as $x^{1/2}$ if the vortex is to be unstable for $x \gg 1$.

At a neutral position, we calculate the local wavenumber $\tilde{k}$ and local Görtler number G_x defined by

$$a_x = \tilde{k} = \sqrt{2x}\, a, \quad G_x = \kappa(x)(2x)^{3/2} \tilde{G} = \tilde{G}. \tag{4.26}$$

By fixing a and varying $\tilde{G}$, we obtain a series of such points $(\tilde{k}, G_x)$ and thus plot a neutral curve. In our calculation, a is fixed at 0.1; the step lengths along x and η directions are taken to be 0.1 and 0.05 respectively; and the lower boundary of the $O(1)$ temperature adjustment layer is taken to be 0.8 while infinity is approximated by 20.8.

In figures 6–12, we have given the results of our numerical calculations. Figure 6 shows five different neutral curves obtained when we use the five different energy measures (4.22)–(4.25) to monitor the energy growth. Figure 7 shows three different neutral curves which are obtained when we impose three different initial conditions at the upstream position $X_0 = 20$, while figure 8 shows three different neutral curves which are obtained when we impose an initial condition at three different upstream locations. In two of these graphs, we have also plotted the two-term asymptotic result (4.19). As we expect, although these neutral curves have distinct left branches, their right branches all converge to the unique large local wavenumber limit. We can see from figure 8 that as the initial location of the disturbance moves towards the leading edge, the neutral curves move progressively

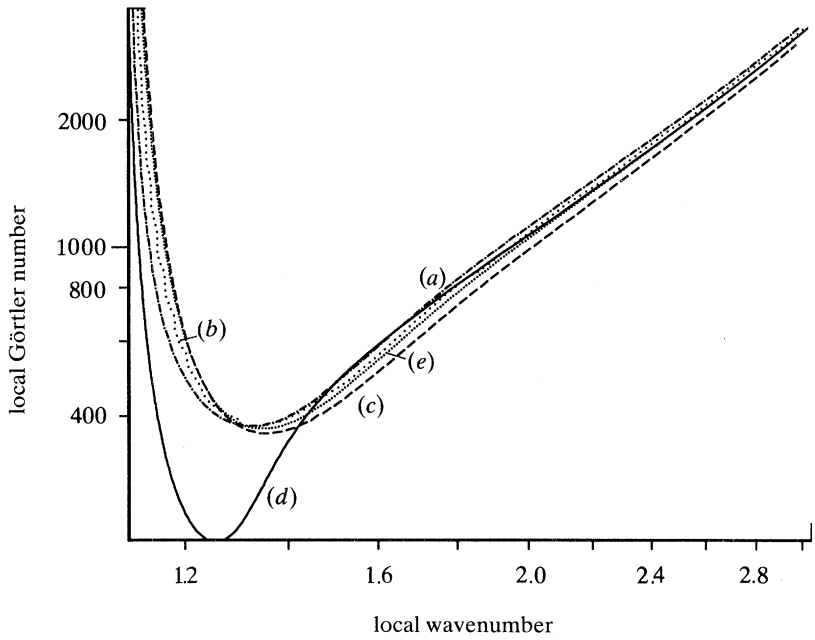

Figure 6. Neutral curves obtained when we impose the following initial conditions at the upstream position, $X_0 = 60$: $\tilde{U} = \mathrm{e}^{-1/\eta^4}\mathrm{e}^{-\eta}/\eta$, $\tilde{V} = 0$, $\tilde{\theta} = \eta\tilde{U}$. Energy measures: (*a*) E_5; (*b*) E_4; (*c*) E_3; (*d*) E_2; (*e*) E_1.

Figure 7

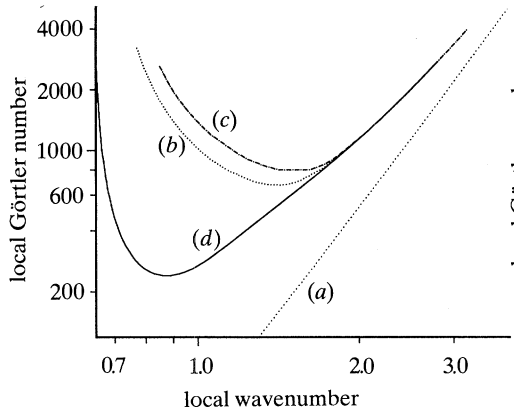

Figure 8

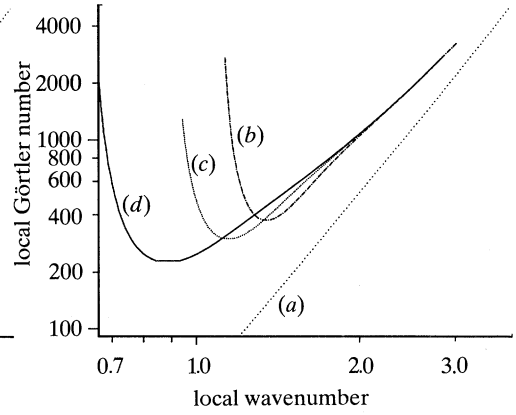

Figure 7. Neutral curves obtained when we impose the following three initial conditions at the downstream location, $X_0 = 20$, and use E_5 as the energy measure to monitor the energy growth: (i) $\tilde{U} = \mathrm{e}^{-1/\eta^4}\mathrm{e}^{-\eta}/\eta$, $\tilde{V} = 0$, $\tilde{\theta} = \eta\tilde{U}$; (ii) $\tilde{U} = \eta^2\mathrm{e}^{-10/\eta^5}\mathrm{e}^{-\eta}$, $\tilde{V} = \mathrm{e}^{-10/\eta^5}\mathrm{e}^{-\eta}$, $\tilde{\theta} = 0$; (iii) $\tilde{U} = \mathrm{e}^{-40/\eta^6}\mathrm{e}^{-\eta}$, $\tilde{V} = \eta^3\mathrm{e}^{-40/\eta^6}\mathrm{e}^{-\eta^2}$, $\tilde{\theta} = 0$. (*a*) Asymptotic result; (*b*) the third initial condition; (*c*) the second initial condition; (*d*) the first initial condition.

Figure 8. Neutral curves obtained when we impose the following initial conditions at three different upstream positions, $X_0 = 20, 40, 60$, and use E_5 as the energy measure: $\tilde{U} = \mathrm{e}^{-1/\eta^4}\mathrm{e}^{-\eta}/\eta$, $\tilde{V} = 0$, $\tilde{\theta} = \eta\tilde{U}$. (*a*) Asymptotic result; (*b*) $X_0 = 60$; (*c*) $X_0 = 20$; (*d*) $X_0 = 40$.

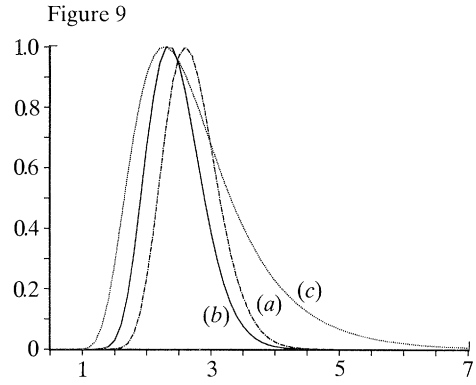

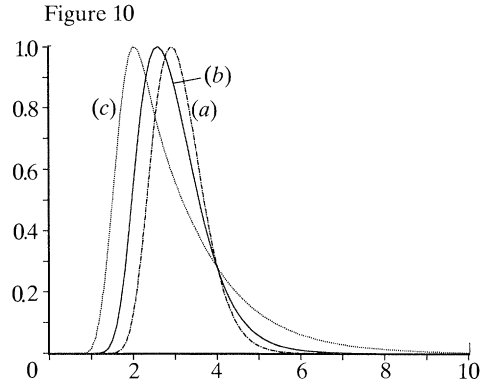

Figure 9. Normalized streamwise velocity at different downstream locations: (*a*) $x = 470$; (*b*) $x = 150$; (*c*) $x = 30$.

Figure 10. Normalized perturbations of V at different downstream locations: (*a*) $x = 470$; (*b*) $x = 150$; (*c*) $x = 30$.

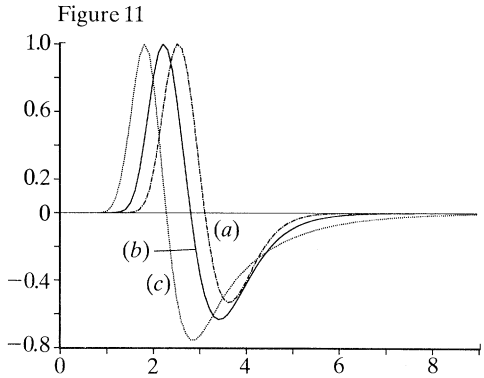

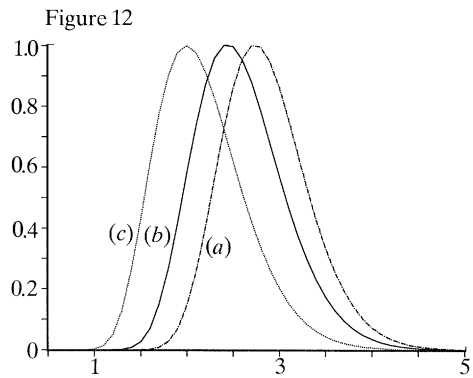

Figure 11. Spanwise velocity perturbation at different downstream locations: (*a*) $x = 470$; (*b*) $x = 150$; (*c*) $x = 30$.

Figure 12. Temperature perturbations at different downstream locations: (*a*) $x = 470$; (*b*) $x = 150$; (*c*) $x = 30$.

up and across to the right. This is contrary to the corresponding results found by Hall (1983) for incompressible flows. Finally, figures 9–12 show the typical profiles of the four perturbation quantities as they evolve downstream, with the initial conditions given by (iii) in figure 7 and $X_0 = 20$, $\tilde{G} = 1000$. To see how the the centre of vortex activity evolves downstream, we have normalized each of the perturbation quantities by its maximum. It is clear that as the vortices evolve downstream (and thus as the local wavenumber increases), they become more and more concentrated, which agrees with the asymptotic result found in

PHILOSOPHICAL TRANSACTIONS OF THE ROYAL SOCIETY A MATHEMATICAL, PHYSICAL & ENGINEERING SCIENCES

the previous subsection that in the large local wavenumber limit, Görtler vortices are trapped in a thin layer of depth $O(\tilde{k}^{-1/2})$ centred at $\eta = 3.001$.

5. Neutral instability with $\kappa(x) \neq (2x)^{-3/2}$

When the wall curvature is not proportional to $(2x)^{-3/2}$, the $O(M^{3/2})$ term on the right-hand side of (3.29) only vanishes at the leading-order neutral position and its effect will persist in the downstream development of Görtler vortices. An important consequence of such an effect is that non-parallel effects will be important over a larger range of wavenumbers than was the case for the special curvature case. Suppose we measure the order of the wavenumber by writing it as $a = O(M^{\alpha})$. Then we show in this section that non-parallel effects continue to be dominant for α up to and including $\frac{1}{4}$. For $\alpha > \frac{1}{4}$, non-parallel effects become negligible compared with viscous effects and an analytical expression can be obtained for the second-order correction to the Görtler number expansion. This second-order correction becomes of the same order as the leading-order term due to the curvature of the basic state when $\alpha = \frac{3}{8}$. In this case a higher-order correction term can also be obtained.

(*a*) $O(1)$ *wavenumber régime: the near neutral inviscid mode*

In the $O(1)$ wavenumber régime, it is convenient to determine the stability properties by considering the evolution of Görtler vortices in the neighbourhood of the leading-order neutral position x_n given by (3.34). Thus we shall fix the Görtler number as given by

$$G = \frac{2B}{(2x_n)^{3/2}\kappa(x_n)} M^{3/2} \tag{5.1}$$

and determine the second-order correction say $\tilde{x}_n$ to the neutral position x_n so that Görtler vortices with G given by (5.1) are neutrally stable at location $x_n + \tilde{x}_n$. Replacing x_n by $x_n - \tilde{x}_n$ in (5.1) then gives the appropriate expansion of the Görtler number for vortices neutrally stable at $x = x_n$.

It can be shown that in the neighbourhood of x_n, the second term in the expansion of $\frac{1}{2}\kappa(x)G$ will force a growth rate of order $M^{1/2}$. Hence we shall consider the evolution of Görtler vortices in an $O(M^{-1/2})$ neighbourhood of x_n by defining a new variable X by

$$X = (x - x_n)M^{1/2}, \tag{5.2}$$

and look for asymptotic solutions of the form

$$\left.\begin{aligned} T = T_0(X,\eta) + \cdots, \quad V = M^{1/2}V_0(X,\eta) + \cdots, \\ W = M^{1/2}W_0(X,\eta) + \cdots, \quad P = MP_0(X,\eta) + \cdots. \end{aligned}\right\} \tag{5.3}$$

Equation (3.29) becomes

$$\bar{u}\bar{v}_x + \bar{v}\bar{v}_y + \tfrac{1}{2}\kappa(x)G\bar{u}^2 = EXM + o(M), \tag{5.4}$$

where

$$E \overset{\text{def}}{=} \left.\frac{\mathrm{d}(G^* - Q)}{\mathrm{d}x}\right|_{x=x_n}. \tag{5.5}$$

Note that it is this term that gives rise to a local growth rate of order $M^{1/2}$. On substituting equations (5.3) into the perturbation equations (3.18)–(3.22), dropping higher-order terms and then eliminating V_0, W_0 and P_0 from the resulting equations in favour of T_0, we find that V_0, W_0 and P_0 are related to T_0 by

$$V_0 = -\frac{\sqrt{2x_n}\,\bar{T}}{\bar{T}'}\frac{\partial T_0}{\partial X}, \tag{5.6}$$

$$\mathrm{i}kW_0 = -\frac{1}{\bar{T}}\frac{\partial V_0}{\partial \eta}, \tag{5.7}$$

$$P_0 = -\frac{\sqrt{2x_n}}{k^2\bar{T}^2}\frac{\partial^2 V_0}{\partial X \partial \eta^2}, \tag{5.8}$$

and that T_0 satisfies the equation

$$\frac{\partial^2}{\partial X^2}\left\{\frac{\partial^2 T_0}{\partial \eta^2} - \frac{2\bar{T}''}{\bar{T}'}\frac{\partial T_0}{\partial \eta} - \left[k^2\bar{T}^2 - \bar{T}\bar{T}'\left(\frac{1}{\bar{T}^2} - \frac{\bar{T}''}{\bar{T}\bar{T}'^2}\right)'\right]T_0\right\} - k^2\frac{EX\bar{T}'}{\sqrt{2x_n}}T_0 = 0, \tag{5.9}$$

where $k \overset{\text{def}}{=} \sqrt{2x_n}\,a$. We can interpret (5.9) as the turning point equation associated with the breakdown of the WKB structure in x of the expansions (3.31), indeed the evolution equation (3.32) is retrieved from (5.9) by taking X to be large. Since this breakdown is associated with a simple zero in x of the right-hand side of (3.32) we expect that the local behaviour of the disturbance should now be expressed in terms of Airy functions. Equation (5.9) admits separable solutions of the form

$$T_0(X,\eta) = \tilde{\phi}(X)\psi(\eta), \tag{5.10}$$

with $\tilde{\phi}$ and ψ satisfying

$$\tilde{\phi}''(X) - \omega X\tilde{\phi}(X) = 0, \tag{5.11}$$

$$\psi''(\eta) - \frac{2\bar{T}''}{\bar{T}'}\psi'(\eta) - \left[k^2\bar{T}^2 - \bar{T}\bar{T}'\left(\frac{1}{\bar{T}^2} - \frac{\bar{T}''}{\bar{T}\bar{T}'^2}\right)'\right]\psi(\eta) - k^2\frac{E\bar{T}'}{\sqrt{2x_n}\omega}\psi(\eta) = 0, \tag{5.12}$$

where the separation constant ω is to be determined by solving the eigenvalue problem (5.12) subject to appropriate boundary conditions. By a simple substitution $z = X\omega^{1/3}$, equation (5.11) reduces to the standard form of Airy's equation $W''(z) - zW(z) = 0$ which has two independent solutions $\mathrm{Ai}(z)$ and $\mathrm{Bi}(z)$, so the solution of (5.11) is given by

$$\tilde{\phi}(X) = a\mathrm{Ai}(\omega^{1/3}X) + b\mathrm{Bi}(\omega^{1/3}X), \tag{5.13}$$

where a and b are two constants to be determined by initial conditions.

To solve (5.12), we first note that in the large wavenumber limit, equation (5.12) takes the same form as equation (3.32). Therefore, the solution of (5.12) can be written in terms of Hermite polynomials as

$$\psi(\eta) = \psi_s = \mathrm{e}^{-\frac{1}{4}\xi^2}He_s(\xi) \tag{5.14}$$

PHILOSOPHICAL TRANSACTIONS OF THE ROYAL SOCIETY A MATHEMATICAL, PHYSICAL & ENGINEERING SCIENCES

and from (3.41) the eigenvalue ω expands as

$$\omega_s = \frac{E}{\sqrt{2x_n}\,\lambda_0}\left(1 - \frac{1}{k}\frac{\lambda_{2s}}{\lambda_0} + \cdots\right), \tag{5.15}$$

where λ_0, λ_{2s} and ξ are defined in turn by (3.43), (3.46) and (3.45 *a*).

In the $O(1)$ wavenumber régime, equation (5.12) has to be solved by a numerical integration, and in general an infinite number of eigenvalues ω_s $(s = 0, 1, \ldots)$ and eigenfunctions ψ_s can be obtained. Then the general solution of (5.9) can be written as

$$T_0 = \sum_{s=0}^{\infty} \{a_s \mathrm{Ai}(\omega_s X) + b_s \mathrm{Bi}(\omega_s X)\}\,\psi_s(\eta), \tag{5.16}$$

where a_s and b_s are constants to be fixed by initial conditions at $X = 0$. From (5.6), V_0 is given by

$$V_0 = -\frac{\sqrt{2x_n}\,\bar{T}}{\bar{T}'} \sum_{s=0}^{\infty} \{a_s \mathrm{Ai}'(\omega_s X) + b_s \mathrm{Bi}'(\omega_s X)\}\,\omega_s \psi_s(\eta). \tag{5.17}$$

It is clear that once $T_0(X, \eta)$ and $V_0(X, \eta)$ are specified at $X = 0$, the coefficients (a_s, b_s) and hence the evolutionary behaviour of the perturbation field (V_0, W_0, T_0, P_0) will be completely determined.

The correction term to the neutral position can be defined as the position where a certain energy measure has zero growth rate. It is obvious that such a position would depend upon what initial conditions we impose at $X = 0$ and what energy measure is used to monitor the energy growth. In principle then it is an easy matter to determine the local neutral position associated with any initial perturbation, we note, however, that before growth of the vortices occurs they will have an oscillatory behaviour in X since both Airy functions are oscillatory on the negative real axis. Clearly this occurs because the boundary between instability and stability is controlled by inviscid effects in this régime, there is no counterpart to this result in the behaviour of Görtler vortices or for that matter Tollmien–Schlichting waves in incompressible flows. We further note that appropriate forms for the initial conditions can be obtained from the receptivity problems associated with wall roughness or free stream disturbances, see Denier *et al.* (1990) and Hall (1990). We merely note in passing here that it is reasonable to expect that the type of mode discussed above is more likely to be stimulated by free-stream disturbances since the effect of wall roughness is diminished by the wall layer over which the wall roughness must diffuse before reaching the unstable adjustment layer.

The non-uniqueness of neutral position mentioned above is certainly typical of the evolution of Görtler vortices in growing boundary layers. In the present problem, non-parallel effects dominate in the evolution of Görtler vortices mainly through the $O(M^{3/2})$ curvature of the basic state. As we increase the wavenumber, viscous effects will gradually come into play in the evolution of Görtler vortices and non-parallel effects will become less important. In the following subsection we consider wavenumbers of order $M^{1/4}$. This is the maximum order at which non-parallel effects are dominant. We shall show that when the wavenumber is increased further above this order, non-parallel effects become negligible.

PHILOSOPHICAL TRANSACTIONS OF THE ROYAL SOCIETY A MATHEMATICAL, PHYSICAL & ENGINEERING SCIENCES

(*b*) *The $O(M^{1/4})$ wavenumber régime: the non-parallel viscous mode*

When the wavenumber reaches the order $M^{1/4}$, the streamwise lengthscale is still $O(M^{-1/2})$ (implying that the local growth rate is $O(M^{1/2})$), but the vertical lengthscale becomes of $O(M^{-1/8})$ (as we expect that vortices would be trapped in an $O(M^{-1/8})$ thin layer). We therefore define two new independent variables X and ξ by

$$X = (x - x_n)M^{1/2}, \quad \xi = (\eta - \eta^*)M^{1/8}, \tag{5.18}$$

where η^* is the centre of vortex activity. For convenience, we define a small parameter ϵ by

$$\epsilon = M^{-1/8}. \tag{5.19}$$

An analysis of the perturbation equations (3.18)–(3.22) shows that

$$V = O(\epsilon^{-4}T), \quad W = O(\epsilon^{-3}T), \quad P = O(\epsilon^{-5}T). \tag{5.20}$$

We now assume that $T = O(1)$ and scale (V, W, P) by $(\epsilon^{-4}, \epsilon^{-3}, \epsilon^{-5})$. Then by neglecting terms of relative order ϵ or higher in the perturbation equations (3.18)–(3.22), we obtain

$$\frac{\partial V}{\partial X} + \hat{a}^2\bar{\mu}_0\bar{T}_0 V - \frac{EX}{\bar{T}_0}T = 0, \tag{5.21}$$

$$\frac{1}{\hat{a}^2}\frac{\partial \bar{W}}{\partial X} - \bar{T}_0 P + \tfrac{4}{3}\bar{\mu}_0\bar{T}_0\bar{W} + \frac{\bar{\mu}_0}{3\sqrt{2x_n}}\frac{\partial V}{\partial \xi} = 0, \tag{5.22}$$

$$\bar{W} = -\frac{1}{\sqrt{2x_n}\,\bar{T}_0}\frac{\partial V}{\partial \xi}, \tag{5.23}$$

$$\frac{V}{\sqrt{2x_n}} = -\frac{\bar{T}_0}{\bar{T}_1}\frac{\partial T}{\partial X} - \frac{\hat{a}^2\bar{\mu}_0\bar{T}_0^2}{\sigma\bar{T}_1}T, \tag{5.24}$$

where $\bar{W} \overset{\text{def}}{=} \mathrm{i}\hat{a}W$, $\hat{a} \overset{\text{def}}{=} M^{-1/4}a$, $\bar{T}_0 = \bar{T}(\eta^*)$, $\bar{T}_1 = \bar{T}'(\eta^*)$, $\bar{\mu}_0 = \bar{\mu}(\bar{T}_0)$ and where we have used the same notation to denote the scaled perturbation quantities. η^* is chosen at higher order such that the vertical structure of T can be expressed in terms of parabolic cylinder functions which vanish at $\eta = \pm\infty$. Elimination of V, $\bar{W}$, and P in favour of T among these equations then gives

$$\frac{\partial^2 T}{\partial X^2} + (1 + \sigma^{-1})\hat{a}^2\bar{\mu}_0\bar{T}_0\frac{\partial T}{\partial X} + \sigma^{-1}\hat{a}^4\bar{\mu}_0{}^2\bar{T}_0{}^2 T + \frac{EX\bar{T}_1}{\sqrt{2x_n}\,\bar{T}_0{}^2}T = 0. \tag{5.25}$$

The solution of the above equation is easily found to be expressible as the product of an Airy function multiplied by $\exp(-\frac{1}{2}X(1 + \sigma^{-1})\hat{a}^2\bar{\mu}_0\bar{T}_0)$. As before the Airy function grows or decays exponentially for large X and is oscillatory on the negative real axis. However, the presence of the exponential factor now leads to a crucial change in the nature of the streamwise evolution of the disturbance. We refer to the fact that the exponential factor, induced by viscous effects, now means that in the stable régime the disturbance decays exponentially rather than oscillating as was the case previously. This result is consistent with the usual result of stability theory that inviscid disturbances change from being oscillatory to being exponential in character when instability occurs; viscous instabilities on the

PHILOSOPHICAL TRANSACTIONS OF THE ROYAL SOCIETY A MATHEMATICAL, PHYSICAL & ENGINEERING SCIENCES

other hand are exponential in nature either side of the stability boundary. The local neutral position can only be obtained by specifying an initial disturbance and finding where the solution of the evolution equation begins to grow.

If we let $\hat{a} \ll 1$, then to leading order equation (5.25) reduces to

$$\frac{\partial^2 T}{\partial X^2} + \frac{EX\bar{T}_1}{\sqrt{2x_n}\,\bar{T}_0^2} T = 0 \tag{5.26}$$

which matches with the asymptotic form of (5.9) when $k \gg 1$.

On the other hand, if we let $\hat{a} \gg 1$, then to leading order (5.25) reduces to

$$\left(\frac{EX\bar{T}_1}{\sqrt{2x_n}\,\bar{T}_0^2} + \frac{1}{\sigma}\hat{a}^4 \bar{\mu}_0^2 \bar{T}_0^2 \right) T = 0, \tag{5.27}$$

which shows that the second-order correction term to the leading-order neutral position becomes independent of non-parallel effects and is given by

$$X = X_n = -\frac{\sqrt{2x_n}}{\sigma E \bar{T}_1} \bar{\mu}_0^2 \bar{T}_0^4 \hat{a}^4, \tag{5.28}$$

On replacing x_n by $x_n - M^{-1/2} X_n$ in (5.1) and expanding the resulting expression in the neighbourhood of x_n, we obtain the following expression for the Görtler number for Görtler vortices neutrally stable at location $x = x_n$:

$$G = \frac{2BM^{3/2}}{\kappa(x_n)(2x_n)^{3/2}} + a^4 \bar{g}_0 + \cdots, \tag{5.29}$$

where

$$\bar{g}_0 = -\frac{2\sqrt{2x_n}\,\bar{\mu}_0^2 \bar{T}_0^4}{\sigma \kappa_0 \bar{T}_1}. \tag{5.30}$$

The expression (5.29) is valid for wavenumbers of order M^α, $\frac{1}{4} < \alpha < \frac{3}{8}$. When the wavenumber reaches the order $M^{3/8}$, the second-order correction term in (5.29) is as large as the first term and a more accurate asymptotic expression can be obtained. That situation will be discussed in the following subsection. We have seen above that in the $O(M^{1/4})$ wavenumber régime viscous effects come into play and modify the evolution of the near neutral inviscid mode, for that reason we refer to the mode in this case as the *non-parallel viscous mode.* We further note that the strongly unstable inviscid mode connects directly with the parallel viscous mode discussed below. Thus we have shown above that the non-parallel viscous mode connects with the near neutral inviscid mode in the vicinity of the right-hand branch of the neutral curve. Hence the initial stages in the evolution of the right-hand branch of the neutral curve are governed by an interplay between viscous and inviscid effects. We further note that, in view of the limiting form (5.29) valid for large a, as the wavenumber increases the neutral Görtler number will also increase.

(*c*) *The $O(M^{3/8})$ wavenumber régime: the parallel viscous mode*

When the wavenumber becomes of order $M^{3/8}$, viscous effects are of the same order as the centrifugal acceleration of the basic state in the determination of the Görtler number, and the leading-order inviscid result (3.35) is to be modified. We

assume that to leading order the Görtler number now expands as

$$G = \frac{2BM^{3/2}}{\kappa(x_n)(2x_n)^{3/2}} + a^4 g_0. \tag{5.31}$$

Here the first term is due to the curvature of the basic state and the second term is due to viscous effects and is to be determined.

For convenience, we introduce a small parameter ϵ and an $O(1)$ constant N by

$$\epsilon \overset{\text{def}}{=} a^{-1}, \quad N \overset{\text{def}}{=} M^{3/2}\epsilon^4, \tag{5.32}$$

so that (5.31) can be written as

$$G = \frac{2BN}{\kappa(x_n)(2x_n)^{3/2}}\frac{1}{\epsilon^4} + \frac{g_0}{\epsilon^4}. \tag{5.33}$$

To determine the higher-order correction terms to the Görtler number expansion, we shall first fix the Görtler number as given by (5.33) and consider the evolution of Görtler vortices in the neighbourhood of the leading-order neutral position x_n defined by (5.31), aiming at finding the second-order correction say $\epsilon\tilde{x}_n$ to the neutral position. As we have remarked at the beginning of the first subsection, replacing x_n by $x_n - \epsilon\tilde{x}_n$ in (5.33) would give the appropriate expansion of the Görtler number for vortices neutrally stable at $x = x_n$.

The vortices under consideration vary on small lengthscales in both x and η directions. In the streamwise direction, their growth rate can be shown to be $O(1/\epsilon)$ so that they evolve on an $O(\epsilon)$ lengthscale. In the η direction, they are confined to an $O(\epsilon^{1/2})$ thin viscous layer because of their small wavelength character. We therefore define two new variables X and ζ by

$$X = \frac{x - x_n}{\epsilon}, \quad \zeta = \frac{\eta - \eta^*}{\epsilon^{1/2}}, \tag{5.34}$$

where η^* is the centre of vortex activity and is to be determined.

We now look for asymptotic solutions of the form

$$\left.\begin{aligned} T &= \theta_0(X,\zeta) + \epsilon^{1/2}\theta_1(X,\zeta) + \epsilon\theta_2(X,\zeta) + \cdots, \\ V &= \epsilon^{-2}[V_0(X,\zeta) + \epsilon^{1/2}V_1(X,\zeta) + \epsilon V_2(X,\zeta) + \cdots], \\ W &= \epsilon^{-3/2}[W_0(X,\zeta) + \epsilon^{1/2}W_1(X,\zeta) + \epsilon W_2(X,\zeta) + \cdots], \\ P &= \epsilon^{-5/2}[P_0(X,\zeta) + \epsilon^{1/2}P_1(X,\zeta) + \epsilon P_2(X,\zeta) + \cdots]. \end{aligned}\right\} \tag{5.35}$$

Here the relative orders of the perturbation quantities are deduced from the perturbation equations (3.18)–(3.22). On inserting these expansions into the perturbation equations (3.18)–(3.22), expanding all coefficients there about $x = x_n$ and $\eta = \eta^*$, and then equating the coefficients of like powers of ϵ, we obtain a hierarchy of equations. To leading order, the Görtler number g_0 in (5.31) is determined as a solvability condition for (V_0, θ_0) and is given by

$$g_0 = -\frac{2\sqrt{2x_n}\,\bar{\mu}_0^2\bar{T}_0^4}{\sigma\kappa_0\bar{T}_1}; \tag{5.36}$$

PHILOSOPHICAL TRANSACTIONS OF THE ROYAL SOCIETY A MATHEMATICAL, PHYSICAL & ENGINEERING SCIENCES

while θ_0, W_0 and P_0 are related to V_0 by

$$\theta_0 = -\frac{\sigma \bar{T}_1}{2\bar{\mu}_0 \bar{T}_0^2 x_n} V_0, \quad \mathrm{i}W_0 = -\frac{1}{\sqrt{2x_n}\,\bar{T}_0}\frac{\partial V_0}{\partial \zeta}, \quad P_0 = -\frac{\bar{\mu}_0}{\bar{T}_0}\frac{\partial V_0}{\partial \zeta}, \tag{5.37}$$

where $\bar{T}_0 = \bar{T}(\eta^*)$, $\bar{T}_1 = \bar{T}'(\eta^*)$, $\bar{\mu}_0 = \bar{\mu}(\bar{T}_0)$, $\kappa_0 = \kappa(x_n)$. Note that (5.36) is of the same form as (5.30), as we would expect.

To next order, we obtain three expressions similar to (5.37) for θ_1, W_1 and P_1 in terms of V_1 and V_0 and the condition that

$$\left.\frac{\mathrm{d}g_0}{\mathrm{d}\eta}\right|_{\eta=\eta^*} = 0, \tag{5.38}$$

which implies that η^* is where g_0 attains its minimum.

If we carry on one order higher, we find from a solvability condition for (V_2, θ_2) that V_0 must satisfy the evolution equation

$$\frac{\partial^2 V_0}{\partial \zeta^2} - \frac{2(1+\sigma)\bar{T}_0 x_n}{3\bar{\mu}_0}\frac{\partial V_0}{\partial X} - \tilde{a}\zeta^2 V_0 + \tilde{b} X V_0 = 0, \tag{5.39}$$

where

$$\tilde{a} = \frac{\bar{T}_0^2 x_n}{3g_0}\left.\frac{\partial^2 g_0}{\partial \eta^2}\right|_{\eta=\eta^*} > 0,$$

$$\tilde{b} = \tfrac{2}{3} x_n \bar{T}_0^2 \left\{\frac{2BN}{g_0\kappa_0(2x_n)^{3/2}}\left(\frac{\kappa_1}{\kappa_0} + \frac{3}{2x_n}\right) + \frac{\kappa_1}{\kappa_0} - \frac{1}{2x_n}\right\}, \tag{5.40}$$

and where $\kappa_1 = \kappa'(x_n)$. The solutions of (5.39) which satisfy the conditions $V_0 \to 0$ as $|\zeta| \to \infty$ can be written as

$$V_0 = V_{0m}(X, \zeta)$$
$$= \exp\left[\frac{3\bar{\mu}_0\tilde{b}}{4(1+\sigma)\bar{T}_0 x_n}\left(X - (m+\tfrac{1}{2})\frac{\sqrt{4\tilde{a}}}{\tilde{b}}\right)^2\right] U(-m-\tfrac{1}{2}, (4\tilde{a})^{1/4}\zeta), \tag{5.41}$$

where $m = 0, 1, 2, \ldots$ and U is a parabolic cylinder function. The neutral position $\tilde{x}_n$ can be taken to be the point where $\partial V_0/\partial X = 0$, so that the mth mode is neutrally stable at

$$X = \tilde{x}_n = (m+\tfrac{1}{2})\sqrt{4\tilde{a}}/\tilde{b}. \tag{5.42}$$

The most unstable mode corresponds to $m = 0$. We therefore have

$$\tilde{x}_n = \sqrt{\tilde{a}}/\tilde{b}. \tag{5.43}$$

With the expression for $\tilde{x}_n$ determined, we can now replace x_n by $x_n - \epsilon\tilde{x}_n$ in (5.33) and then expand the two terms on the right-hand side up to and including the $O(1/\epsilon^3)$ term, hence obtaining the expansion

$$G = \frac{2BM^{3/2}}{\kappa(x_n)(2x_n)^{3/2}} + \frac{g_0}{\epsilon^4} + \frac{1}{\epsilon^3}\frac{1}{\sqrt{2x_n}}\sqrt{\frac{3g_0}{2\bar{T}_0^2}\frac{\partial^2 g_0}{\partial \eta^{*2}}} + \cdots. \tag{5.44}$$

for Görtler vortices which are neutrally stable at position x_n.

As is to be expected, the Görtler number expansion (5.44) agrees in the special

PHILOSOPHICAL TRANSACTIONS OF THE ROYAL SOCIETY A MATHEMATICAL, PHYSICAL & ENGINEERING SCIENCES

case $\kappa = (2x)^{-3/2}$ with the combination of (4.1), (4.10 *a*), (4.12 *d*) and (4.17) (note that the small parameter ϵ there corresponds to $\epsilon/\sqrt{2x_n}$ here). This means that in the large wavenumber limit, the relation (5.44) is a universal expression for the neutral Görtler number, which is valid for all wall curvatures.

Finally in this subsection we stress that a more unstable version of the parallel viscous mode can be obtained by taking g_0 bigger than the value given by (5.36), in that case we must allow for a growth rate of order $M^{3/4}$ and then (5.36) is replaced by an equation to determine that growth rate. This structure then enables a direct connection between the strongly unstable inviscid mode and the parallel viscous mode at relatively high Görtler numbers with $G - G_N \sim M^{3/2}$. The analysis for this more unstable régime is essentially identical to that given by Denier *et al.* (1990) in the incompressible case.

6. The wall layer mode

It has been established in § 3 that as the wavenumber becomes large, Görtler vortices become increasingly trapped in the $O(1)$ temperature adjustment layer. Thus the preceding three sections are devoted to Görtler vortices which have wavelength of $O(1)$ or smaller and which are trapped in the temperature adjustment layer. Clearly it is possible for vortices of wavelength smaller than the thickness of the adjustment layer to be excited, far enough downstream the local wavenumber will become comparable with the adjustment layer thickness and the previous analysis will apply. However, before this occurs the vortices must be described by an analysis which takes account of the fact that they are of wavelength much larger than the adjustment layer thickness, we shall now address that situation. In fact it can be deduced from the definition (2.10) and (3.1 *c*) that the variation $\mathrm{d}y$ of the physical variable y and the variation of the similarity variable $\mathrm{d}\eta$ satisfy

$$\mathrm{d}y = \sqrt{2x}\,\bar{T}\,\mathrm{d}\eta. \tag{6.1}$$

The wall layer which corresponds to $\eta = O(M^{-1/2})$ with $\bar{T} = O(M^2)$ is therefore actually of $O(M^{3/2})$ thickness in terms of the physical variable y, while the temperature adjustment layer is still of $O(1)$ thickness. Thus a natural scale for larger wavelength vortices is provided by the thickness of the wall layer, the appropriate size of the Görtler number is found by rescaling the vortex wavelength and velocity field by the scales relevant to the wall layer. Such Görtler vortices are referred to as the *wall mode* and are studied in the present section to complete our stability analysis.

Since in the large Mach number limit the boundary layer thickens by $O(M^{3/2})$, we should rescale (y, z) by a factor $M^{3/2}$ and the corresponding velocity components likewise. This effectively replaces $R^{-1/2}$ by $R^{-1/2}M^{3/2}$. It is therefore appropriate to rescale the Görtler number G and the wavenumber a by defining

$$\tilde{G} = M^{-3/2}\kappa(x)(2x)^{3/2}G, \quad \tilde{k} = \sqrt{2x}\,M^{3/2}a. \tag{6.2}$$

In the wall layer, the basic state is from (2.11) and (3.5) given by

$$\bar{u} = F'(Y), \quad \bar{v} = \frac{M^{3/2}}{\sqrt{2x}}[-\tilde{T}F(Y) + F'(Y)\Omega(Y)], \tag{6.3}$$

where

$$\Omega(Y) \overset{\text{def}}{=} \int_0^Y \tilde{T}\,\mathrm{d}Y. \tag{6.4}$$

The various partial derivatives of u, v and μ which appear in the perturbation equations (3.18)–(3.22) have to be computed before we can deduce the relative orders of the perturbation quantities. Such expressions are given in the Appendix A to this paper. With the aid of these expressions, we can show from (3.18)–(3.22) that the relative scalings of the velocity, pressure and temperature disturbance fields are given by

$$V = O(M^{3/2}U), \quad W = O(M^{3/2}U), \quad T = O(M^2U), \quad P = O(MU). \tag{6.5}$$

We therefore look for solutions of the form

$$\left.\begin{aligned} U &= \tilde{U}(x,Y) + \cdots, \quad V = M^{3/2}\tilde{V}(x,Y) + \cdots, \\ W &= M^{3/2}\tilde{W}(x,Y) + \cdots, \quad P = M^2\tilde{P}(x,Y) + \cdots, \\ T &= M^2\tilde{\theta}(x,Y) + \cdots. \end{aligned}\right\} \tag{6.6}$$

On substituting (6.6) into the perturbation equations (3.18)–(3.22) and then equating the coefficients of like powers of M, we obtain to leading order a set of partial differential equations for $\tilde{U}$, $\tilde{V}$, $\tilde{W}$, $\tilde{P}$ and $\tilde{\theta}$ which govern the evolution of Görtler vortices in the wall layer. For the purpose of numerical calculation, it is convenient to eliminate the pressure perturbation $\tilde{P}$ and $\tilde{W}$ from these equations. After some manipulation, we obtain

$$\begin{aligned} \frac{\partial^2\tilde{U}}{\partial Y^2} - \frac{F'\sqrt{\tilde{T}}}{1+\tilde{m}}(2x)\frac{\partial\tilde{U}}{\partial x} &= \frac{\sqrt{2x}\,F''}{(1+\tilde{m})\sqrt{\tilde{T}}}\tilde{V} - \frac{F''}{2\tilde{T}}\frac{\partial\tilde{\theta}}{\partial Y} + \left(\frac{\tilde{T}'}{2\tilde{T}} - \frac{F\sqrt{\tilde{T}}}{1+\tilde{m}}\right)\frac{\partial\tilde{U}}{\partial Y} \\ &+ \left\{\frac{FF''}{(1+\tilde{m})\sqrt{\tilde{T}}} - \tfrac{1}{2}\sqrt{\tilde{T}}\left(\frac{F'''}{\tilde{T}^{3/2}} - \frac{3F''\tilde{T}'}{2\tilde{T}^{5/2}}\right)\right\}\tilde{\theta} + \left\{\tilde{k}^2\tilde{T}^2 - \frac{F''\Omega}{(1+\tilde{m})\sqrt{\tilde{T}}}\right\}\tilde{U}, \end{aligned} \tag{6.7}$$

$$\begin{aligned} \frac{\partial^2\tilde{\theta}}{\partial Y^2} - \frac{\sigma F'\sqrt{\tilde{T}}}{1+\tilde{m}}(2x)\frac{\partial\tilde{\theta}}{\partial x} &= -\frac{\sigma F\sqrt{\tilde{T}}}{1+\tilde{m}}\frac{\partial\tilde{\theta}}{\partial Y} + \frac{\sigma\tilde{T}'}{(1+\tilde{m})\sqrt{\tilde{T}}}\sqrt{2x}\tilde{V} - \frac{\sigma\Omega\tilde{T}'}{(1+\tilde{m})\sqrt{\tilde{T}}}\tilde{U} \\ &- 2\sigma(\gamma-1)F''\frac{\partial\tilde{U}}{\partial Y} + \left\{\tilde{k}^2\tilde{T}^2 + \frac{\sigma F\tilde{T}'}{(1+\tilde{m})\sqrt{\tilde{T}}} - \tfrac{1}{2}\sigma(\gamma-1)\frac{F''^2}{\tilde{T}} - \frac{\tilde{T}''}{2\tilde{T}} + \frac{3\tilde{T}'^2}{4\tilde{T}^2}\right\}\tilde{\theta}, \end{aligned} \tag{6.8}$$

$$\begin{aligned} \frac{\partial^4\tilde{V}}{\partial Y^4} - \frac{F'\sqrt{\tilde{T}}}{1+\tilde{m}}(2x)\frac{\partial^3\tilde{V}}{\partial x\partial Y^2} + \left(\frac{3\tilde{T}'F'}{\tilde{T}} - F''\right)\frac{\sqrt{\tilde{T}}}{1+\tilde{m}}(2x)\frac{\partial^2\tilde{V}}{\partial x\partial Y} \\ + \frac{F'}{1+\tilde{m}}\left(\frac{F''\tilde{T}'}{\sqrt{\tilde{T}}\,F'} - \frac{3\tilde{T}'^2}{\tilde{T}^{3/2}} + \frac{\tilde{T}''}{\sqrt{\tilde{T}}} + \tilde{k}^2\tilde{T}^{5/2}\right)(2x)\frac{\partial\tilde{V}}{\partial x} = \sum_{i=1}^{4} b_i, \end{aligned} \tag{6.9}$$

where the expressions for b_i are given in Appendix C to this paper.

The above equations are to be solved subject to the following boundary conditions.

At $Y = 0$,

$$\left.\begin{aligned} \tilde{U} = \tilde{V} = \partial\tilde{V}/\partial Y = 0, \\ \partial\tilde{\theta}/\partial Y = 0, \quad \text{if the wall is thermally insulated,} \\ \tilde{\theta} = 0, \quad \text{if the wall is under cooling.} \end{aligned}\right\} \tag{6.10}$$

As $Y \to \infty$,

$$\tilde{U} \to 0, \quad \tilde{V} \to 0, \quad \partial\tilde{V}/\partial Y \to 0, \quad \tilde{\theta} \to 0. \tag{6.11}$$

The precise large Y decay behaviour of the perturbation quantities can be deduced from the perturbation equations (6.7)–(6.9), but the derivation is tedious. However, the far downstream limit of such decay behaviour can be deduced very easily from the condition that the solutions of the wall mode under consideration in the double limit $\tilde{k} \to \infty$ and $Y \to \infty$ should match with the inviscid solutions (3.32) and (3.33) when $\tilde{k} \to 0$ and $\eta \to \infty$ there. In the limit $\tilde{k} \to 0$, equation (3.32) reduces to equation (3.37) and the latter has solutions confined to a thin layer $\eta = O(\tilde{k}^{1/3})$ near the wall. It can be shown that in the further limit $\eta \to \infty$, the solution of (3.37) has

$$V_0 \to c_1 + c_2/\eta^7, \tag{6.12}$$

and from (3.33),

$$T_0 \to (c_3/\eta)V_0, \quad W_0 \to c_4/\eta^4, \tag{6.13}$$

where c_1, c_2, c_3 and c_4 are all functions of x. To match with the above solutions, $\tilde{V}$ should decay like Y^{-7}, $\tilde{\theta}$ like Y^{-8} and $\tilde{W}$ like Y^{-4}.

For any initial disturbance located at a given downstream position, we can determine the position at which the disturbance becomes neutrally stable by integrating these equations using the same marching procedure as the one used in solving the system of equations (4.3)–(4.7). As an illustrative example, we impose the following initial disturbance at the location $x = 50$:

$$\tilde{U}(50, Y) = Y^5 \mathrm{e}^{-Y^3}, \quad \tilde{V}(50, Y) = \tilde{\theta}(50, Y) = 0. \tag{6.14}$$

The wall curvature is taken to be $\sqrt{2x}$ and the wall is assumed to be thermally insulated. For a given wavenumber and a given Görtler number, we can march downstream until we reach the neutral position where a certain energy measure has zero growth rate. We then calculate the local wavenumber $\tilde{k}$ and the local Görtler number $\tilde{G}$ at the neutral position. By fixing the wavenumber a $(= \tilde{k}(2x)^{-1/2})$ at 1 and varying the Görtler number $M^{-3/2}G$ from 0.0001 to 0.03, we obtain a series of neutral points $(\tilde{k}, \tilde{G})$. Figure 13 shows the neutral curves corresponding to the following three energy measures:

$$E_1 = \int_0^\infty \tilde{U}^2 \,\mathrm{d}y = \sqrt{2x}\, M^{3/2} \int_0^\infty \tilde{U}^2 \tilde{T} \,\mathrm{d}Y, \tag{6.15}$$

$$E_2 = \int_0^\infty (\tilde{U}^2 + \tilde{V}^2 + \tilde{W}^2) \,\mathrm{d}y = \sqrt{2x}\, M^{3/2} \int_0^\infty (\tilde{U}^2 + \tilde{V}^2 + \tilde{W}^2)\tilde{T} \,\mathrm{d}Y, \tag{6.16}$$

$$E_3 = \int_0^\infty \left(\frac{\partial\tilde{U}}{\partial y}\right)^2 \mathrm{d}y = \frac{M^{-3/2}}{\sqrt{2x}} \int_0^\infty \frac{1}{\tilde{T}} \left(\frac{\partial\tilde{U}}{\partial Y}\right)^2 \mathrm{d}Y. \tag{6.17}$$

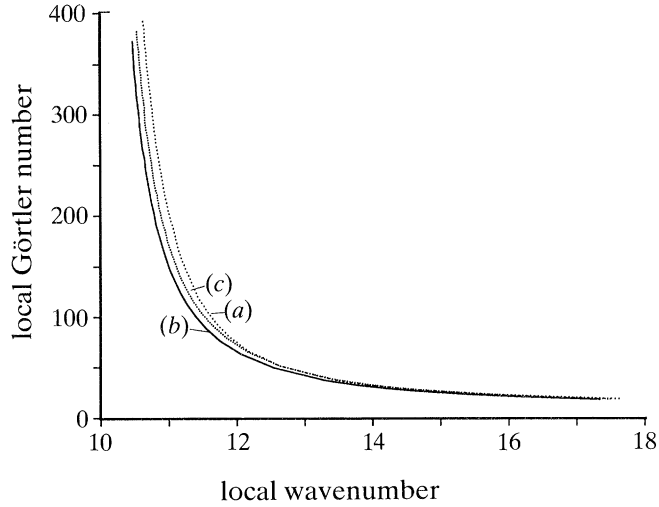

Figure 13. Neutral curves for the acoustic mode; energy measures: (*a*) E_3; (*b*) E_2; (*c*) E_1.

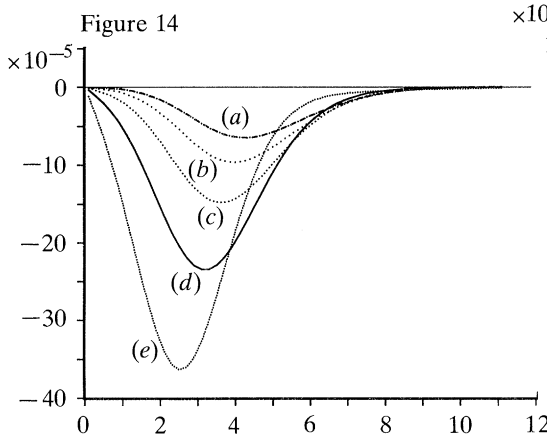

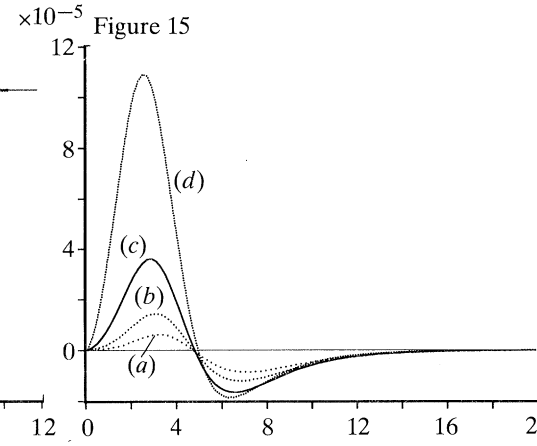

Figure 14. U perturbation at different downstream locations: (*a*) $x = 160$; (*b*) $x = 140$; (*c*) $x = 120$; (*d*) $x = 100$; (*e*) $x = 80$.

Figure 15. V perturbation at different downstream locations: (*a*) $x = 140$; (*b*) $x = 120$; (*c*) $x = 100$; (*d*) $x = 80$.

Figures 14–17 shows the downstream evolution of Görtler vortices corresponding to the above conditions with $M^{-3/2}G = 0.001$. We observe that all neutral curves decrease monotonically with respect to the local wavenumber and that Görtler vortices become increasingly more and more shifted to the right (i.e. towards the temperature adjustment layer) as they evolve downstream. This is certainly to be expected since in the large local wavenumber limit the wall mode has to match with the mode trapped in the temperature adjustment layer. By taking the large wavenumber limit of the wall mode equations we can show that the neutral curve should tend to the limit $\tilde{G} = 2B = 1.2543$. To realize this limit numerically we have to carry out our calculation at very large wavenumbers. This presents some numerical difficulties, because on one hand, if we fix the Görtler

PHILOSOPHICAL TRANSACTIONS OF THE ROYAL SOCIETY A MATHEMATICAL, PHYSICAL & ENGINEERING SCIENCES

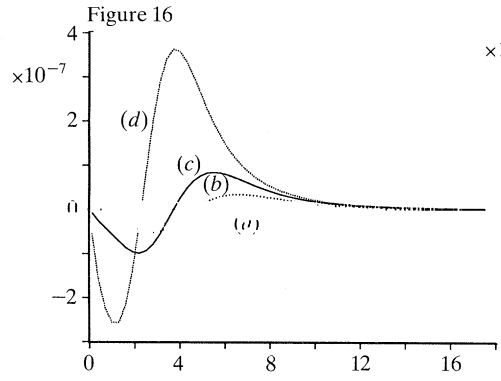

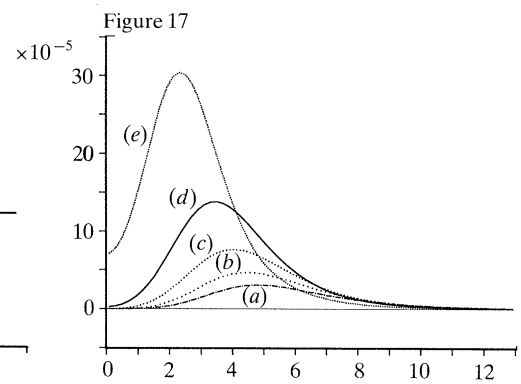

Figure 16. W perturbation at different downstream locations: (*a*) $x = 120$; (*b*) $x = 100$; (*c*) $x = 80$; (*d*) $x = 60$.

Figure 17. Temperature perturbation at different downstream locations: (*a*) $x = 140$; (*b*) $x = 120$; (*c*) $x = 100$; (*d*) $x = 80$; (*e*) $x = 60$.

number and vary the wavenumber, the initial conditions soon become incompatible with the differential equations since for large wavenumbers Görtler vortices have to be trapped in a region away from the wall; on the other hand, if we fix the wavenumber and vary the Görtler number, a large local wavenumber corresponds to a large downstream neutral position and there contamination from the 'finite infinity' becomes important because of the algebraic decay behaviour (implying that we have to choose a larger infinity). Finally, we remark that the x-derivative of $\tilde{\theta}$ in the expressions for W_3 and $\bar{W}$ defined in Appendix C could be eliminated with the aid of equation (6.8) to give a different formulation and thus to provide a check on our numerical scheme. We have done so and have obtained identical results.

We conclude this section by stating the most important results of our investigation of the wall mode. We have shown that the wall layer can support a disturbance trapped in the wall layer with wavelength comparable with the wall layer thickness. This mode is dominated by non-parallel effects and has a neutral Görtler number which is a monotonic decreasing function of the vortex wavenumber. In the limit of high vortex wavenumbers the mode takes on a structure essentially identical to that found for the small wavenumber limit of the inviscid modes of wavelength comparable with the adjustment layer thickness. Moreover in this limit the vortex has a neutral Görtler number which approaches from above the zero-order approximation to the neutral Görtler number of the mode trapped in the temperature adjustment layer.

7. Real gas effects

In our previous discussions, we have assumed that the fluid under consideration is an ideal gas undergoing no dissociation. Our asymptotic analysis based on the large Mach number limit has yielded some revealing results about the stability properties of hypersonic boundary layers. However, in the large Mach number limit, we would expect that the wall temperature should be well above the temperature at which dissociation takes place. Take a boundary layer over a

PHILOSOPHICAL TRANSACTIONS OF THE ROYAL SOCIETY A MATHEMATICAL, PHYSICAL & ENGINEERING SCIENCES

thermally insulated wall as an example. The temperature at the wall is given by

$$T_{\mathrm{w}} = \tfrac{1}{2}(\gamma - 1)M^2 T_\infty$$

when the Prandtl number is unity. At a standard altitude of 53 km, the air temperature T_∞ is 283 K. If we take $\gamma = 1.4$, $M = 15$, then $T_{\mathrm{w}} = 12\,735$ K.

Since at the far lower temperature of 2500 K, the oxygen molecules in the air have already begun to dissociate, it is clear that an investigation which takes gas dissociation into account is vitally important!

A complete theory on real gas effects should at least incorporate the following important chemical reactions:

$$\mathrm{O_2} \rightleftharpoons 2\mathrm{O}, \qquad \mathrm{N_2} \rightleftharpoons 2\mathrm{N},$$

$$\mathrm{N} + \mathrm{O} \rightleftharpoons \mathrm{NO}, \qquad \mathrm{N} + \mathrm{O} \rightleftharpoons \mathrm{NO^+} + \mathrm{e^-}.$$

However, to expose the most important features and at the same time keep the algebra to a minimum, we begin our investigation by eliminating the less essential complications which arise from the detailed composition of air and confining our attention to a pure dissociating diatomic gas. The dissociation process is therefore denoted by

$$\mathrm{A_2} \rightleftharpoons \mathrm{A} + \mathrm{A}. \tag{7.1}$$

In our following discussion, $\mathrm{O_2}$ and $\mathrm{N_2}$ will be chosen for numerical illustration. Furthermore, we assume that the fluid under consideration is an *ideal dissociating gas* which satisfies the relation

$$\frac{\alpha^2}{1-\alpha^2} = \frac{p_{\mathrm{d}}}{p}\frac{T}{T_{\mathrm{d}}}\mathrm{e}^{-T_{\mathrm{d}}/T} \tag{7.2}$$

(see Becker (1968, p. 36), or Lighthill (1957, p. 6)). Here α, p and T have the same meanings as defined in § 2, while p_{d} and T_{d} are respectively the *characteristic pressure* and *temperature* for dissociation.

For the gas mixture of A and $\mathrm{A_2}$, Dalton's law gives

$$p = p_1 + p_2 = \frac{n_1 \Re T}{V} + \frac{n_2 \Re T}{V}, \tag{7.3}$$

where p_i is the pressure which the ith component would exert individually if alone in volume V at temperature T, n_i are mole numbers and $\Re$ is the universal gas constant. Here we use subscript 1 to signify component gas $\mathrm{A_2}$ and subscript 2 for A. Assume that the mass of a mole of gas A is m, the molar mass of gas $\mathrm{A_2}$ is then $2m$. We therefore have

$$\rho = \frac{n_1 \cdot 2m + n_2 \cdot m}{V}, \tag{7.4}$$

$$\alpha = \frac{n_2 \cdot m}{n_1 \cdot 2m + n_2 \cdot m} = \frac{n_2}{2n_1 + n_2}. \tag{7.5}$$

With the use of (7.4) and (7.5), we can rewrite the equation of state (7.3) as

$$p = (1 + \alpha)\bar{\Re}\rho T, \tag{7.6}$$

where $\bar{\Re} = \Re/(2m)$ is a gas constant.

Table 2.

	T_d/K	P_d/atoms	$\rho_d/(\mathrm{g\,cm^{-3}})$
oxygen	59 000	2.3×10^7	150
nitrogen	113 000	4.1×10^7	130

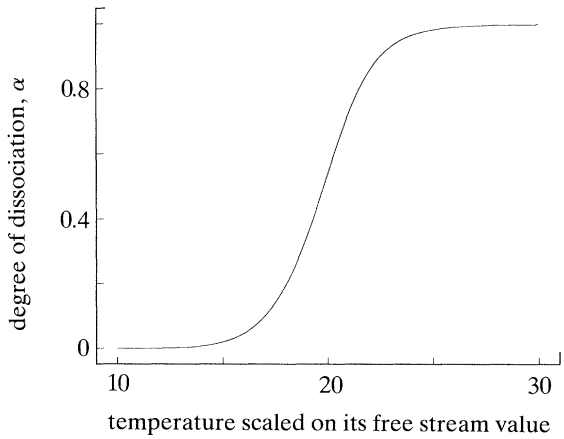

Figure 18. Variation of α with respect to the temperature.

On inserting (7.6) into (7.2), we obtain

$$\frac{\alpha^2}{1-\alpha} = \frac{\rho_d}{\rho} e^{-T_d/T}, \tag{7.7}$$

where $\rho_d = P_d/(\bar{\mathfrak{R}} T_d)$ is the *characteristic density* for dissociation. ρ_d, P_d and T_d are in general functions of T, but their variations over a large temperature range are very slight. Their typical values are given in table 2 (taken from Lighthill 1957).

It should be noted that for atmospheric values of ρ, ρ_d/ρ is at least 10^5. Thus although ρ_d, T_d and p_d are called characteristic quantities, they are not typical of the actual values of ρ, T and p at all. For $\rho_d/\rho = 10^5$, (7.7) shows that α is 0.05 (5% dissociation) when $T/T_d = 0.057$, and α is 0.95 (95% dissociation) when $T/T_d = 0.116$. For densities typical of the upper atmosphere, with (say) $\rho_d/\rho = 10^7$, these values of T/T_d would be reduced to 0.045 and 0.076 respectively. For fixed values of $\rho_d/\rho_\infty = 10^7$ and $T_d/T_\infty = 4 \times 10^2$, the variation of α with respect to T/T_∞ is plotted in figure 18.

Relation (7.7) was first obtained by Lighthill (1957) from quantum mechanics, and therefore the ideal dissociating gas discussed here is also called the Lighthill gas. Using a purely mathematical argument, Becker (1968) has shown that the Lighthill gas is a special case of a more general class of gases. An important property of Lighthill gases is that A_2 and A have the same specific heats at constant volume, that is,

$$c_{v1} = c_{v2}. \tag{7.8}$$

(*a*) *Constitutive properties of a dissociating gas*

To see the complications which arise from gas dissociation, let us first recall that an ideal gas has the following properties which have greatly simplified our previous analysis.

1. The equation of state has the simple form $P = \bar{\Re}\rho T$ as compared with (7.6).
2. Specific heats c_p and c_v can be taken to be constant.
3. The coefficient of thermal conduction k is proportional to the shear viscosity μ and the Prandtl number $\sigma = \mu c_p/k$ is usually taken to be constant.
4. The viscosity can be taken to be related to the temperature by Chapman's law, or more accurately, by Sutherland's law.

When part of an ideal gas has been dissociated, the gas becomes a mixture of two-component gases and all of the above properties are changed. We have shown above that the equation of state is modified to the form given by (7.6). In this subsection, we derive the corresponding expressions for μ, k and c_p. Our derivation is based on work discussed in *The mathematical theory of non-uniform gases* by Chapman & Cowling (1970).

(i) *The viscosity* μ

In the kinetic theory of gases, different expressions for the transport properties μ and k have been found depending on what model is used for the interaction of the gas molecules. For example, for a simple gas which consists of smooth rigid elastic spherical molecules, μ is proportional to $\sqrt{T}$, while if the gas is taken to consist of smooth rigid elastic spherical molecules each of which is surrounded by a field of attractive force, μ is given by

$$\mu = \frac{5}{16c^2}\left(\frac{\Re m T}{\pi}\right)^{1/2} \Big/ \left(1 + \frac{S}{T}\right), \tag{7.9}$$

where c is the diameter of the molecule, S the potential energy of the mutual attraction of two molecules when in contact, m the molecular mass. Relation (7.9) is known as Sutherland's viscosity law.

For a binary mixture of gases, Wilke's law gives an approximate expression for the viscosity of the mixture:

$$\mu = x_1 \Big/ \left(\frac{x_1}{\mu_1} + \frac{x_2}{\mu_{12}}\right) + x_2 \Big/ \left(\frac{x_1}{\mu_{21}} + \frac{x_2}{\mu_2}\right), \tag{7.10}$$

where μ_1 and μ_2 are the viscosities of the two-component gases; x_1 and x_2 denote the proportions by volume of the two gases in the mixture. Since by Avogadro's law equal volumes of different gases contain an equal number of molecules or moles, we have

$$x_1 = \frac{n_1}{n_1 + n_2} = \frac{1-\alpha}{1+\alpha}, \quad x_2 = \frac{n_2}{n_1 + n_2} = \frac{2\alpha}{1+\alpha}. \tag{7.11}$$

In (7.10), μ_{12} and μ_{21} are the mutual viscosities of the two-component gases and are given by

$$\mu_{12} = \frac{5m_1}{16c_{12}^2}\left[\frac{\Re T(m_1+m_2)}{2\pi m_1 m_2}\right]^{1/2} \Big/ \left(1 + \frac{S_{12}}{T}\right), \quad \mu_{21} = \frac{m_2}{m_1}\mu_{12} = \tfrac{1}{2}\mu_{12}, \tag{7.12}$$

where c_{12} can be taken to be $\frac{1}{2}(c_1 + c_2)$, while the expression for S_{12} has to be found empirically. Lindsay & Bromley (1950) suggested that $S_{12} = \sqrt{S_1 S_2}$. Here c_i and S_i $(i = 1, 2)$ are constants appearing in (7.9), associated with μ_i.

With the aid of (7.9) and (7.12), we can now write down the appropriate expressions for the viscosities of the component gases. These are

$$\mu_i = \frac{A_i T^{3/2}}{T + S_i}, \quad i = 1, 2, \quad \mu_{12} = \frac{A_3 T^{3/2}}{T + S_{12}}, \quad \mu_{21} = \tfrac{1}{2}\mu_{12}, \tag{7.13}$$

Here

$$A_i = \frac{5}{16 c_i^2}\sqrt{\frac{\Re m_i}{\pi}}, \quad A_3 = \frac{5}{16 c_{12}^2}\sqrt{\frac{3\Re m_i}{\pi}}, \tag{7.14}$$

where we have made use of the fact that $m_1 = 2m_2$.

(ii) *Coefficient of thermal conduction k*

For a pure gas, the coefficient of thermal conduction is related to the viscosity μ by the simple formula

$$k = f c_v \mu, \tag{7.15}$$

where f is a constant and γ/f is usually defined as the Prandtl number.

For a binary gas mixture, Wassiljewa's formula gives

$$k = x_1 \Big/ \left(\frac{x_1}{k_1} + \frac{x_2}{k_{12}}\right) + x_2 \Big/ \left(\frac{x_1}{k_{21}} + \frac{x_2}{k_2}\right), \tag{7.16}$$

where k_1 and k_2 are the thermal conductivities of the two- component gases and k_{12}, and k_{21} are the mutual thermal conductivities.

It is suggested in Chapman & Cowling (1970, p. 256) to put

$$\frac{k_1}{k_{12}} = \alpha_{12}\frac{D_{11}}{D_{12}}, \quad \frac{k_2}{k_{21}} = \alpha_{21}\frac{D_{22}}{D_{12}}, \tag{7.17}$$

where the coefficients α_{12} and α_{21} are regarded as functions of m_1/m_2, which are determined semi-empirically, and for Sutherland's model the diffusion coefficients D_{11}, D_{12} and D_{22} are given by

$$D_{11} = \frac{6}{5\rho_1}\mu_1, \quad D_{12} = \frac{6}{5\rho_1}\mu_{12}, \quad D_{22} = \frac{6}{5\rho_2}\mu_2, \tag{7.18}$$

where ρ_i is the density of the ith-component gas, when pure, at the pressure and temperature of the actual mixture.

If we take $\alpha_{12} = \alpha_{21} = 1$ for simplicity and further make use of the above relations, relation (7.16) then becomes

$$k = c_v f_1 \left\{\mu_1 \Big/ \left(1 + \frac{x_2}{x_1}\frac{\mu_1}{\mu_{12}}\right) + \frac{f_2}{f_1}\mu_2 \Big/ \left(1 + \frac{2x_1}{x_2}\frac{\mu_2}{\mu_{12}}\right)\right\}, \tag{7.19}$$

where we have used the fact that for an ideal dissociating gas, $c_{v1} = c_{v2} \stackrel{\text{def}}{=} c_v$; while f_1 and f_2 are the constants appearing in (7.15) corresponding to gases A_2 and A respectively.

PHILOSOPHICAL TRANSACTIONS OF THE ROYAL SOCIETY A MATHEMATICAL, PHYSICAL & ENGINEERING SCIENCES

For easy comparison, we rewrite (7.10) here, making use of the relation (7.12),

$$\mu = \mu_1 \Big/ \left(1 + \frac{x_2}{x_1}\frac{\mu_1}{\mu_{12}}\right) + \mu_2 \Big/ \left(1 + \frac{2x_1}{x_2}\frac{\mu_2}{\mu_{12}}\right). \tag{7.20}$$

Comparing (7.19) with (7.20) shows that we can almost write $k = c_v f_1 \mu$ for the gas mixture, only if $f_2 = f_1$. It is therefore desirable to investigate the values of f_1 (for diatomic gases) and f_2 (for monatomic gases).

For all smooth spherically symmetrical molecules, it has been shown that taking $f_2 = 2.5$ provides a very good approximation. However, for diatomic and polyatomic gases, a variety of expressions have been suggested for f. One of these is Eucken's formula:

$$f = \tfrac{1}{4}(9\gamma - 5). \tag{7.21}$$

This formula is valid under the assumption that the transport of momentum and translational energy is unaffected by the internal molecular motions, and that internal energy is transported at the same rate as momentum.

For diatomic gases, there are three translational degrees of freedom, two rotational degrees of freedom and on the average one vibrational degree of freedom (may vary between zero and two depending on whether vibration has been fully excited or not). Thus the internal energy is given by

$$e_1 = \frac{1}{2}\frac{\Re T}{(2m)}(3 + 2 + 1) = \frac{3\Re T}{2m}, \tag{7.22}$$

(Recalling that $2m$ is the molecular mass of A_2.) Consequently, the specific heats are

$$c_{v1} = \frac{\partial e_1}{\partial T} = \frac{3\Re}{2m}, \quad c_{p1} = c_{v1} + \frac{\Re}{2m} = \frac{2\Re}{m}. \tag{7.23}$$

We then have

$$\gamma = c_{p1}/c_{v1} = \tfrac{4}{3} = 1.33, \quad f = \tfrac{7}{4} = 1.75. \tag{7.24}$$

At lower temperatures when the vibrational mode is not excited,

$$e_1 = \tfrac{5}{2}(\Re T/2m), \quad c_{v1} = \tfrac{5}{2}(\Re/2m), \quad c_{p1} = \tfrac{7}{2}(\Re/2m),$$

and therefore

$$\gamma = \tfrac{7}{5} = 1.4, \quad f = 1.90.$$

At the other limit when the vibrational mode is fully excited,

$$e_1 = \tfrac{7}{2}(\Re T/2m), \quad c_{v1} = \tfrac{7}{2}(\Re/2m), \quad c_{p1} = \tfrac{9}{2}(\Re/2m),$$

and hence

$$\gamma = \tfrac{9}{7} = 1.29, \quad f = 1.68.$$

Therefore, in general,

$$1.68 < f < 1.90. \tag{7.25}$$

In passing, we note that for monatomic gases, there are only three translational degrees of freedom and therefore

$$e_2 = 3 \times \tfrac{1}{2}\Re T/m = \tfrac{3}{2}\Re T/m. \tag{7.26}$$

Comparing (7.26) with (7.22) then shows that monatomic and diatomic gases

PHILOSOPHICAL TRANSACTIONS OF THE ROYAL SOCIETY A MATHEMATICAL, PHYSICAL & ENGINEERING SCIENCES

have internal energies differing only on their zero point energies and that the basic assumption $c_{v1} = c_{v2}$ for an ideal dissociating gas is indeed valid. Also, the f value 2.5 for a monatomic gas can actually be read off from Eucken's formula (7.21) by noting that $c_{v2} = 3\Re/(2m)$, $c_{p2} = 5\Re/(2m)$ and $\gamma = \frac{5}{3}$.

We now return to (7.19). From the above discussion, it is appropriate to put $c_v = 3\Re/(2m)$, $f_1 = \frac{7}{4}$, $f_2 = \frac{5}{2}$. The coefficient of thermal conduction k for the mixture is then given by the formula

$$k = \frac{21\Re}{8m}\left\{\mu_1 \Big/ \left(1 + \frac{x_2}{x_1}\frac{\mu_1}{\mu_{12}}\right) + \tfrac{10}{7}\mu_2 \Big/ \left(1 + \frac{2x_1}{x_2}\frac{\mu_2}{\mu_{12}}\right)\right\}. \tag{7.27}$$

(iii) *Specific heats of the mixture*

The specific internal energy for A and A_2 both have the same expression

$$e = 3\Re T/2m.$$

The total internal energy of the mixture is then given by

$$E = \frac{3\Re T}{2m}(2m \cdot n_1 + m \cdot n_2). \tag{7.28}$$

Since A and A_2 do not necessarily have the same zero-point energy, relation (7.28) should be modified to

$$E = \frac{3\Re T}{2m}(2m \cdot n_1 + m \cdot n_2) + \tfrac{1}{2}\Re T_{\mathrm{d}} n_2, \tag{7.29}$$

where the last term represents the difference of zero-point energies of A over A_2.

On dividing (7.29) by the total mass of the mixture $(2mn_1 + mn_2)$, we obtain the expression for the specific internal energy of the mixture:

$$e = 3\bar{\Re}T + \bar{\Re}T_{\mathrm{d}}\alpha. \tag{7.30}$$

With the aid of this relation and the equation of state (7.6), we can easily calculate the specific enthalpy as follows:

$$h = e + p/\rho = (4 + \alpha)\bar{\Re}T + \bar{\Re}T_{\mathrm{d}}\alpha. \tag{7.31}$$

To calculate specific heats, we have to first of all evaluate $(\partial\alpha/\partial T)_\rho$ and $(\partial\alpha/\partial T)_p$. From (7.7),

$$\left(\frac{\partial\alpha}{\partial T}\right)_\rho = \frac{T_{\mathrm{d}}}{T^2}\frac{\alpha(1-\alpha)}{2-\alpha}, \quad \left(\frac{\partial\alpha}{\partial T}\right)_p = \frac{1}{T}\left(1 + \frac{T_{\mathrm{d}}}{T}\right)\cdot\tfrac{1}{2}\alpha(1-\alpha^2). \tag{7.32}$$

It then follows from (7.30) and (7.31) that

$$\left.\begin{aligned} c_v &= \left(\frac{\partial e}{\partial T}\right)_v = 3\bar{\Re} + \bar{\Re}\left(\frac{T_{\mathrm{d}}}{T}\right)^2\frac{\alpha(1-\alpha)}{2-\alpha}, \\ c_p &= (4+\alpha)\bar{\Re} + \tfrac{1}{2}\bar{\Re}(1 + T_{\mathrm{d}}/T)^2\alpha(1-\alpha^2). \end{aligned}\right\} \tag{7.33}$$

The quantity $(\partial h/\partial p)_T$ which appears in (2.7) can now be calculated with the use of (7.31) and (7.2). The result is

$$\left(\frac{\partial h}{\partial p}\right)_T = -\frac{\bar{\Re}(T + T_{\mathrm{d}})}{2p}\alpha(1-\alpha^2) = -\frac{1}{2\rho}\left(1 + \frac{T_{\mathrm{d}}}{T}\right)\alpha(1-\alpha). \tag{7.34}$$

(*b*) *Modification of the basic state*

As we have remarked before, the basic state equations (2.12) and (2.13) are independent of constitutive assumptions and therefore also valid for the gas mixture under consideration, although now $\bar{\rho}$, $\bar{\mu}$, $\bar{k}$ and $\bar{c}_p$ are calculated from the more complicated expressions (7.6), (7.10), (7.27) and (7.33), respectively. In these expressions, the function α is given by (7.7). After non-dimensionalization, these equations become

$$\bar{\rho} = 1/(1+\alpha)\bar{T}, \tag{7.35}$$

$$\bar{\mu} = \frac{(1+\tilde{m}_1)\bar{T}^{3/2}}{\bar{T}+\tilde{m}_1+\tilde{A}_3^{-1}2\alpha(1-\alpha)^{-1}(\bar{T}+\tilde{m}_3)} + \frac{\tilde{A}_2(1+\tilde{m}_1)\bar{T}^{3/2}}{\bar{T}+\tilde{m}_2+\tilde{A}_2\tilde{A}_3^{-1}\alpha^{-1}(1-\alpha)(\bar{T}+\tilde{m}_3)}, \tag{7.36}$$

$$\bar{k} = \frac{(1+\tilde{m}_1)\bar{T}^{3/2}}{\bar{T}+\tilde{m}_1+\tilde{A}_3^{-1}2\alpha(1-\alpha)^{-1}(\bar{T}+\tilde{m}_3)} + \frac{\frac{10}{7}\tilde{A}_2(1+\tilde{m}_1)\bar{T}^{3/2}}{\bar{T}+\tilde{m}_2+\tilde{A}_2\tilde{A}_3^{-1}\alpha^{-1}(1-\alpha)(\bar{T}+\tilde{m}_3)}, \tag{7.37}$$

$$\bar{c}_p = 1 + \tfrac{1}{4}\alpha + \tfrac{1}{8}(1+T_{\mathrm{d}}/\bar{T}_\infty T)^2\alpha(1-\alpha^2), \tag{7.38}$$

$$\frac{\alpha^2}{1-\alpha^2} = \frac{\rho_{\mathrm{d}}}{\rho_\infty}\bar{T}\exp\left(-\frac{T_{\mathrm{d}}}{T_\infty\bar{T}}\right), \tag{7.39}$$

where

$$\left.\begin{aligned} \tilde{m}_1 &= \frac{S_1}{T_\infty}, \quad \tilde{m}_2 = \frac{S_2}{T_\infty}, \quad \tilde{m}_3 = \frac{\sqrt{S_1S_2}}{T_\infty}, \\ \tilde{A}_2 &= \frac{A_2}{A_1} = \frac{c_1^2}{\sqrt{2}c_2^2}, \quad \tilde{A}_3 = \frac{A_3}{A_1} = \sqrt{\frac{3}{2}}\frac{c_1^2}{c_{12}^2}. \end{aligned}\right\} \tag{7.40}$$

For the purpose of asymptotic analysis, it is convenient to define two new constants a and b by

$$a = \frac{\rho_{\mathrm{d}}}{\rho_\infty}M^2, \quad b = \frac{T_{\mathrm{d}}}{T_\infty M^2}. \tag{7.41}$$

Then equation (7.39) becomes

$$\frac{\alpha^2}{1-\alpha^2} = \frac{a\bar{T}}{M^2}\mathrm{e}^{-bM^2/\bar{T}}, \tag{7.42}$$

which displays the physical fact that dissociation will take place in the hottest region where $\bar{T} = O(M^2)$.

An asymptotic analysis of equations (2.12) and (2.13) shows that the boundary layer structure in the present case is similar to that for an ideal gas. In particular, the boundary layer can be divided into two regions: an inner region $\eta = O(M^{-1/2})$ and a temperature adjustment region $\eta = O(1)$. In the inner region, we define new variables Y, $\tilde{T}$ as in (3.5), but now (3.6) and (3.7) are replaced by

$$(1+\tilde{m}_1)\left(\frac{h_1(\alpha)}{1+\alpha}\frac{F''}{\sqrt{\tilde{T}}}\right)' + FF'' = 0, \tag{7.43}$$

$$\frac{1+\tilde{m}_1}{\sigma}\left(\frac{h_2(\alpha)}{1+\alpha}\frac{\tilde{T}'}{\sqrt{\tilde{T}}}\right)' + \bar{c}_p F\tilde{T}' + (\gamma-1)(1+\tilde{m}_1)\frac{h_1(\alpha)}{1+\alpha}\frac{(F'')^2}{\sqrt{\tilde{T}}} = 0, \tag{7.44}$$

where

$$h_1 \overset{\text{def}}{=} \frac{\tilde{A}_3(1-\alpha)}{2\alpha+\tilde{A}_3(1-\alpha)} + \frac{\tilde{A}_2\tilde{A}_3\alpha}{\tilde{A}_3\alpha+\tilde{A}_2(1-\alpha)}, \tag{7.45}$$

$$h_2 \overset{\text{def}}{=} \frac{\tilde{A}_3(1-\alpha)}{2\alpha+\tilde{A}_3(1-\alpha)} + \frac{\frac{10}{7}\tilde{A}_2\tilde{A}_3\alpha}{\tilde{A}_3\alpha+\tilde{A}_2(1-\alpha)}, \tag{7.46}$$

$$\bar{c}_p = 1 + \tfrac{1}{4}\alpha + \tfrac{1}{8}(1+b/\tilde{T})^2\cdot\alpha(1-\alpha^2), \tag{7.47}$$

and where α satisfies

$$\frac{\alpha^2}{1-\alpha^2} = a\tilde{T}\mathrm{e}^{-b/\tilde{T}}. \tag{7.48}$$

As $Y\to\infty$, $\tilde{T}\to 0$ and we expect that $\alpha\to 0$. From (7.45), (7.46) and (7.38) we have $h_1\to 1$, $h_2\to 1$ and $\bar{c}_p\to 1$. Equations (7.43) and (7.44) can then be approximated by

$$(1+\tilde{m}_1)\left(F''/\sqrt{\tilde{T}}\right)' + FF'' = 0, \tag{7.49}$$

$$\sigma^{-1}(1+\tilde{m}_1)\left(\tilde{T}'/\sqrt{\tilde{T}}\right)' + F\tilde{T}' + (\gamma-1)(1+\tilde{m}_1)(F'')^2/\sqrt{\tilde{T}} = 0, \tag{7.50}$$

which have asymptotic solution

$$F = Y-\beta+\frac{D}{(Y-\beta)^{3/\sigma}}+\cdots, \quad \tilde{T} = \left[\frac{3(1+\tilde{m}_1)}{\sigma}\right]^2\frac{1}{(Y-\beta)^4}+\ldots, \tag{7.51}$$

where both D and β are constants. Therefore, equations (7.43) and (7.44) are to be solved subject to the boundary conditions (3.8) and the asymptotic conditions (7.51). Results from such a numerical integration are shown in figure 1 together with those results corresponding to the undissociated model.

In the temperature adjustment layer $\eta = O(1)$, α is exponentially small which means that no dissociation takes place in this region. The basic state equations (2.12) and (2.13) reduce to (3.13) and (3.14) which are appropriate for an ideal gas and which are to be solved subject to the same matching conditions (3.15) and the conditions (3.16) at infinity.

(*c*) *Modification of the stability properties*

Since the boundary layer structure is similar to that for an ideal gas when dissociation is taken into account, the qualitative stability properties are also similar with appropriate quantitative modifications. In particular, we can still show that the mode trapped in the temperature adjustment layer is most susceptible to Görtler vortices and the neutral Görtler number expands as in (3.35), but now the coefficient B is modified since it is the leading-order contribution to the integration of basic state temperature across the whole boundary layer. As for higher-order correction terms to the Görtler number expansion, The effect of gas dissociation is dependent on the wall curvature. In the special curvature case, since the second term $\tilde{G}$ in (4.1) is determined by solving partial differential

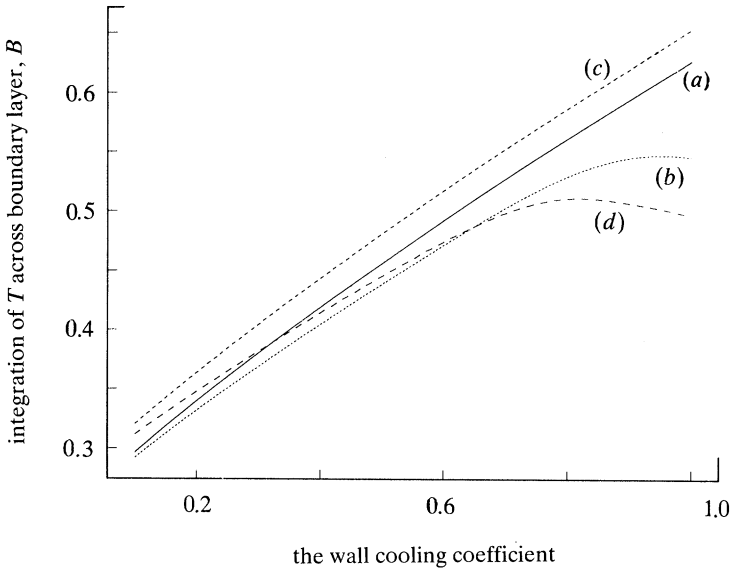

Figure 19. Dependence of B on the wall cooling coefficient. (*a*) $\sigma = 0.72$, ideal gas; (*b*) $\sigma = 0.72$, real gas; (*c*) $\sigma = 1.00$, ideal gas; (*d*) $\sigma = 1.00$, real gas.

equations in the undissociated temperature adjustment layer, it is not affected by consideration of gas dissociation; while in the more general curvature case, we can see from (5.9) that gas dissociation affects the second-order correction term through E, but in the higher wavenumber case discussed in § 5 *c*, the second-order correction term is not affected by gas dissociation, as is clear from (5.44).

In figure 19, we have plotted the variation of B with respect to the cooling coefficient both for the real gas model discussed here and for the ideal gas model used in § 3. It is clear from figure 19 that the values of B is decreased by gas dissociation as well as by wall cooling. Therefore, both gas dissociation and wall cooling are destabilizing. In our numerical integration of the boundary layer equations (7.43) and (7.44), we have taken

$$\tilde{m}_1 = \tilde{m} = 0.508, \quad \tilde{A}_2 = \tilde{A}_3 = 1, \quad a = 1.21 \times 10^9, \quad b = 3.30$$

(these values for a and b correspond to $M = 11$ if $\rho_{\mathrm{d}}/\rho_\infty = 10^7$, $T_{\mathrm{d}} = 1.13 \times 10^5$, and $T_\infty = 283$). We have also repeated our calculation for a few sets of different values for the above five constants. We find that the above prediction is still valid.

To determine the effects of gas dissociation on the wall mode, we have integrated the perturbation equations (6.7)–(6.9) with the basic state given by the solutions of (7.49) and (7.50), subject to the same conditions as those used to produce the neutral curves in figure 13. Figures 20–22 give a comparison of the neutral curves corresponding to the ideal gas model and the real gas model with dissociation. We observe that in each of these figures, the two neutral curves corresponding to the two models intersect. Therefore, gas dissociation can have either a stabilizing effect or a destabilizing effect on the wall mode.

Figure 20

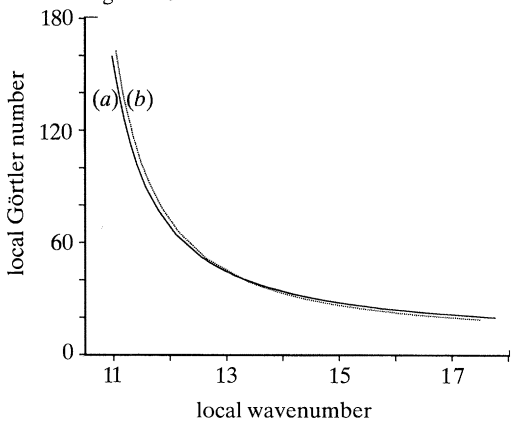

Figure 21

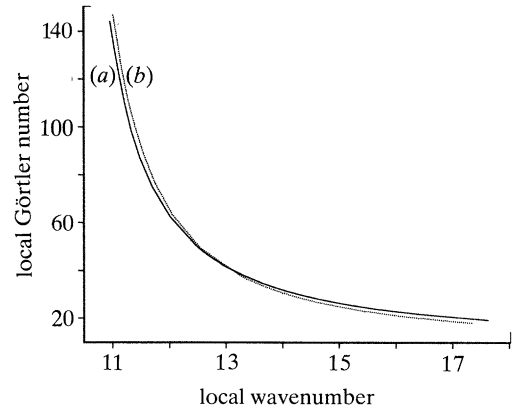

Figure 20. A comparison of neutral curves corresponding to (*a*) the real gas model, and (*b*) the ideal gas model. The energy measure is E_1.

Figure 21. A comparison of neutral curves corresponding to (*a*) the real gas model, and (*b*) the ideal gas model. The energy measure is E_2.

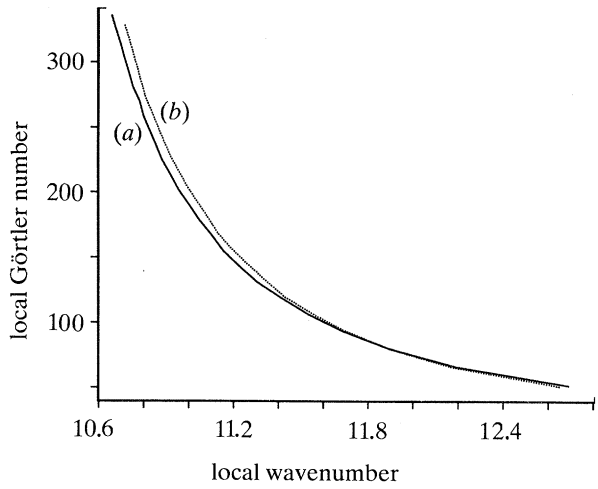

Figure 22. A comparison of neutral curves corresponding to (*a*) the real gas model, and (*b*) the ideal gas model. The energy measure is E_3.

8. Further discussion

We have seen above that the Görtler mechanism in a hypersonic boundary layer of a Sutherland law fluid behaves in a predominantly viscous or inviscid manner depending on whether or not the wall curvature varies like $x^{-3/2}$ where x denotes distance along the wall. When the wall curvature does not have this special form the vortices evolve over almost the whole of the wavenumber space in a non-parallel manner subject to viscous effects. The only exception to this case is at extremely high wavenumbers where the vortices evolve in a quasi-parallel manner essentially identical to that described for incompressible flows by Hall (1982). Since the special curvature distribution is possibly of little physical

PHILOSOPHICAL TRANSACTIONS OF THE ROYAL SOCIETY A MATHEMATICAL, PHYSICAL & ENGINEERING SCIENCES

Table 3.

mode	wavenumber	growth rate	neutral value of G
wall	$O(M^{-3/2})$	$O(1)$	$O(M^{3/2}) + \cdots$
strongly unstable inviscid	$O(1)$	$O(M^{3/4})$	no neutral G
near neutral inviscid	$O(1)$	$O(M^{1/2})$	$G_N + O(M) + \cdots$
non-parallel viscous	$O(M^{1/4})$	$O(M^{1/2})$	$G_N + O(M) + \cdots$
parallel viscous	$O(M^{3/8})$	$O(M^{3/4})$	$O(M^{3/2}) + \cdots$

relevance we shall now concentrate on the results we have found for the more general curvature situation.

The results we have found for the different wavenumber régimes for the general curvature distribution are summarized in table 3 (G_N is as defined in the text following equation (3.35)).

The wall mode which was discussed in § 6 is in fact the counterpart of the so-called 'acoustic mode' of the inviscid hypersonic instability theory of flat plate boundary layers. The latter Rayleigh instability has been discussed by Cowley & Hall (1990) and Smith & Brown (1990) for Chapman law fluids, and a limited discussion of this mode for Sutherland law fluids can be found in Blackaby *et al.* (1993). The acoustic mode and the wall mode discussed in § 6 have the property that they are concentrated in the wall layer where the streamwise velocity component of the basic state varies from zero at the wall to almost its free-stream value. The Rayleigh acoustic mode in general evolves in a quasi-parallel manner though in the presence of strong shocks this is not necessarily the case. The wall mode discussed in this paper evolves in a non-parallel manner and becomes progressively concentrated towards the edge of the wall layer as the local wavenumber increases.

When the wavenumber of the vortex becomes $O(1)$ then the disturbance modifies itself so as to become concentrated in the adjustment layer where the basic state temperature adjusts rapidly to its free-stream value. The counterpart of this mode in the Rayleigh instability problem is the so-called 'vorticity' mode discussed for Chapman law fluids by Smith & Brown (1990) and subsequently for Sutherland law fluids by Blackaby *et al.* (1993). We found in the present paper that when the Görtler number G is as given by (3.27) with $G^* > Q$ and Q given by (3.28), then the appropriate expansion of the disturbance field is given by (3.31). Thus the mode has growth rate $O(M^{3/4})$ and the growth rate is given by the solution of the eigenvalue problem specified by (3.32) subject to the condition that V_0 should vanish at $0, \infty$. Figure 3 shows that the growth rate increases monotonically from zero as the wavenumber increases and tends to a constant at large wavenumbers. At large wavenumbers the growth rate can be matched onto the parallel viscous mode growth rate when the vortex wavenumber becomes formally $O(M^{3/8})$. We note here that the inviscid mode matches directly onto the parallel viscous mode structure at sufficiently high Görtler numbers. This is exactly the situation with the inviscid–viscous connection between temporally growing Görtler vortices in incompressible flows and is a direct consequence of the fact that the growth rate of the inviscid mode shown in figure 3 tends to a constant at large values of the wavenumber. In the corresponding spatially growing problem

Figure 23

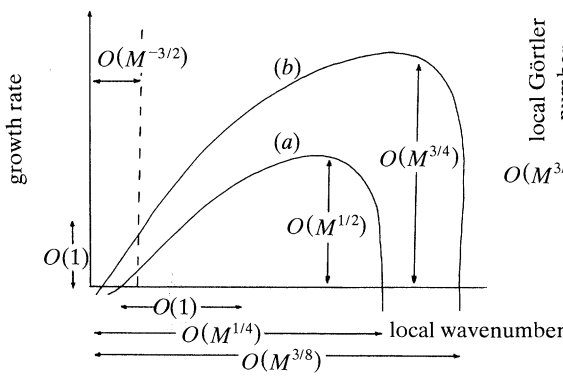

Figure 24

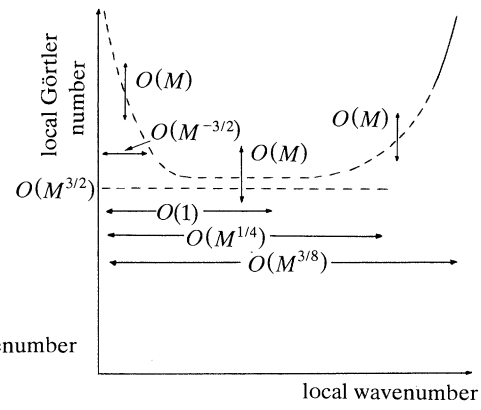

Figure 23. The growth rate structure for Görtler vortices in hypersonic boundary layers. (*a*) The near neutral régime; (*b*) the strongly unstable régime.

Figure 24. The neutral curve for Görtler vortices in hypersonic boundary layers. The dashed part of the curve indicates that at the given wavenumbers the curve depends at zero order on non-parallel effects. The vertical arrows indicate the size of the next order correction to the neutral curve; apart from the régime where the wavenumber is $O(M^{3/8})$ the correction depends on non-parallel effects.

for incompressible flows Denier *et al.* (1990) show that an intermediate region is required to make the inviscid–viscous connection and indeed that the maximum possible growth rate is achieved in that interval. We stress that this intermediate régime has no connection with the non-parallel viscous mode discussed in § 5. The latter régime is appropriate only to the inviscid–viscous connection problem at mildly supercritical values of G. In figure 23 we have sketched the dependence of the growth rate on the wavenumber for the cases when the Görtler number is mildly supercritical (i.e. when G differs only slightly from its value required to overcome the strong $O(M^{3/2})$ curvature of the basic state) and the strongly unstable case with $G \sim O(M^{3/2})$. The broken parts of the curve denote régimes where the growth rate is given by a non-parallel calculation. In figure 24 we sketch the neutral curve in the (local Görtler number)–(local wavenumber) plane. In this figure we have indicated the corrections to the neutral curve associated with non-parallel effects.

There are no available experimental results with which we can compare with our calculations, this is because experiments at the high Mach numbers, say 10–30, appropriate to our work are exceedingly difficult to perform. Thus for design purposes it is fair to say that a theoretical approach is the only means at this stage to predict the likely evolution of Görtler vortices in growing hypersonic boundary layers. Current transition prediction methods are all based on some amplitude growth criterion based on the linear growth of a disturbance. We have seen above that for a realistic hypersonic boundary layer the régime where vortex growth is likely to occur is the strongly unstable inviscid one. Hence in any transition prediction method for a hypersonic boundary layer it would be appropriate to

simply compute the local Görtler number and obtain the corresponding growth rate from figure 3; this of course should only be done for wavenumbers less than the neutral value associated with parallel viscous mode structure. However, it should be noted that faster growing travelling wave disturbances might be more important in the transition process.

Finally we close by making a few remarks about the results of § 7 which concerned the effect of gas dissociation and wall cooling on vortex growth. First let us make a few remarks about the effect of wall cooling, since the most unstable vortices correspond to the strongly unstable inviscid mode we concentrate on that situation. In that case the main effect of wall cooling or real gas effects is to alter the quantity B which fixes the scaled Görtler number above which instability can occur. Figure 19 shows that for an ideal gas the effect of wall cooling is to reduce B by a factor of about 0.5 when the wall temperature is cooled from its adiabatic value by a factor of 10. We find that the eigenvalue problem associated with (3.32) has the maximum value of β altered only by a small amount when this happens so that at a given value of the Görtler number the growth rate is increased by a factor of about 1.4 when the wall temperature is reduced by a factor of 10 from its adiabatic value. By contrast real gas effects have a negligible impact on the growth rate of the strongly unstable mode. Thus for example in figure 19 we see that, at a fixed value of the cooling coefficient, B varies by only about 10 % when the real gas model is used. Thus the critical Görtler number or the disturbance growth rate is altered only slightly by real gas effects so it would seem that any transition prediction method could quite sensibly ignore such a complication; certainly the error associated with doing so would be negligible compared with the inherent error of the prediction method.

We thank Dr Philip Wadey for his advice concerning the computations of § 6 and Dr M. Malik for comments regarding real gas effects. This research was supported in part by the National Aeronautics and Space Administration under NASA Contract no. NAS1-18605 while the second author was in residence at the Institute for Computer Applications in Science and Engineering (ICASE), NASA Langley Research Center, Hampton, VA 23665. This work was also partly supported by NASA under Grant NASA 18107 and by USAF under Grant AFOSR89-0042.

Appendix A. Basic state properties

Listed here are various derivatives related to the basic state, which are used frequently in the determination of the relative orders of the perturbation quantities.

(*a*) *The temperature adjustment layer*

$$\bar{u} = f'(\eta) = 1 + \frac{\hat{f}'(\eta)}{M_1} + \cdots, \quad \bar{v} = \frac{1}{\sqrt{2x}}\left(-\bar{T}f + f'\int_0^\eta \bar{T}\,\mathrm{d}\eta\right) = \frac{B}{\sqrt{2x}}M^{3/2} + \cdots, \tag{A 1}$$

$$\eta_{,x} = -\frac{1}{2x\bar{T}}\int_0^\eta \bar{T}\,\mathrm{d}\eta = -\frac{B}{2x\bar{T}}M^{3/2} + \cdots, \qquad \eta_{,y} = \frac{1}{\sqrt{2x}\,\bar{T}}, \tag{A 2}$$

$$\bar{u}_x = -\frac{B\hat{f}''(\eta)}{2x\bar{T}}\frac{M^{3/2}}{M_1} + \cdots, \qquad \bar{u}_y = \frac{\hat{f}''(\eta)}{\sqrt{2x}\,\bar{T}}\frac{1}{M_1} + \cdots, \tag{A 3}$$

$$\bar{v}_x = -(2x)^{-3/2}(1-\eta\bar{T}'/\bar{T})BM^{3/2}+\cdots, \qquad \bar{v}_y = -\eta\bar{T}'/2x\bar{T}+\cdots, \tag{A 4}$$

$$\bar{u}\frac{\partial}{\partial x}+\bar{v}\frac{\partial}{\partial y} = \frac{\partial}{\partial x}-\frac{\eta}{2x}\frac{\partial}{\partial \eta}+\cdots,$$

$$\bar{u}\bar{v}_x+\bar{v}\bar{v}_y = -(2x)^{-3/2}[BM^{3/2}+\bar{\mu}\bar{T}'/\sigma\bar{T}-\eta^2\bar{T}']+\cdots. \tag{A 5}$$

(b) *The wall layer*

$$\bar{u} = F'(Y), \quad \bar{v} = \frac{M^{3/2}}{\sqrt{2x}}[-\tilde{T}F+F'(Y)\Omega(Y)], \tag{A 6}$$

$$\eta_x = -\frac{M^{-1/2}}{2x\tilde{T}}\Omega(Y), \quad \eta_y = \frac{M^{-2}}{\sqrt{2x}\,\tilde{T}}, \tag{A 7}$$

$$Y_x = -\frac{1}{2x\tilde{T}}\Omega(Y), \quad Y_y = \frac{M^{-3/2}}{\sqrt{2x}\,\tilde{T}}, \tag{A 8}$$

$$\bar{u}_x = F''(Y)Y_x, \quad \bar{u}_y = F''(Y)Y_y, \tag{A 9}$$

$$\bar{v}_x = -M^{3/2}(2x)^{-3/2}[-\tilde{T}F+(F'-\tilde{T}'F/\tilde{T})\Omega+(F''/\tilde{T})\Omega^2], \tag{A 10}$$

$$\bar{v}_y = (2x\tilde{T})^{-1}[-\tilde{T}'F+F''\Omega], \tag{A 11}$$

$$\bar{u}\frac{\partial}{\partial x}+\bar{v}\frac{\partial}{\partial y} = F'\frac{\partial}{\partial X}-\frac{F}{2x}\frac{\partial}{\partial Y}, \tag{A 12}$$

$$\bar{u}\bar{v}_x+\bar{v}\bar{v}_y = -M^{3/2}(2x)^{-3/2}[-\tilde{T}FF'-\tilde{T}'F^2+(F'^2+FF'')\Omega], \tag{A 13}$$

$$\bar{u}\bar{u}_x+\bar{v}\bar{u}_y = -FF''/2x, \tag{A 14}$$

where

$$\Omega(Y) \overset{\text{def}}{=} \int_0^Y \tilde{T}\,\mathrm{d}Y. \tag{A 15}$$

Appendix B. Expressions for a_i appearing in (4.20)

$$a_1 = \eta\tilde{k}^2\bar{T}\frac{\partial^2\tilde{\theta}}{\partial\eta^2}, \quad a_2 = \tilde{k}^2\left[\frac{2\tilde{\mu}}{\bar{\mu}}\eta\bar{T}\bar{T}'-\eta\bar{T}'+\frac{1}{\mu}\eta^2\bar{T}^2\right]\frac{\partial\tilde{\theta}}{\partial\eta},$$

$$a_3 = -\tilde{k}^2\left\{(1-\sigma^{-1})\bar{T}'+\eta\bar{T}''-\frac{\eta\bar{T}'^2}{\bar{T}}-\frac{2\bar{T}}{\bar{\mu}}(\tilde{\mu}'\eta\bar{T}'+\tilde{\mu}\bar{T}'+\tilde{\mu}\eta\bar{T}'')\right.$$
$$\left.+\frac{2\tilde{\mu}}{\bar{\mu}}\eta\bar{T}'^2+\frac{\eta\bar{T}^2}{\bar{\mu}}+\frac{2\eta^2\bar{T}\bar{T}'}{\bar{\mu}}+\frac{\bar{T}}{2\bar{\mu}}\tilde{G}\right\}\tilde{\theta},$$

$$a_4 = \left\{ -\frac{\tilde{k}^2 \bar{T}\bar{T}'}{\bar{\mu}} \left[\tilde{\mu}' + \frac{1}{3}\left(\frac{\tilde{\mu}\bar{T}'}{\bar{T}} - \frac{\bar{\mu}\bar{T}'}{\bar{T}^2} \right) - \tilde{k}^2 \left(\frac{\tilde{\mu}}{\bar{\mu}} + \frac{1}{3\bar{T}} \right) (\bar{T}''\bar{T} - \bar{T}'^2) \right] \right.$$

$$\left. -\tilde{k}^2 \left(\frac{\tilde{\mu}}{\bar{\mu}} - \frac{1}{\bar{T}} \right) \bar{T}'^2 + \tfrac{4}{3}\tilde{k}^2 \left(\frac{\tilde{\mu}}{\bar{\mu}} \bar{T}'^2 + \bar{T}'' - \frac{2\bar{T}'^2}{\bar{T}} \right) + \frac{2\tilde{k}^2}{\bar{\mu}} \eta \bar{T}\bar{T}' - \tilde{k}^4 \bar{T}^3 \right\} (-\tilde{V}),$$

$$a_5 = -\frac{3\bar{T}'}{\bar{T}^2} \frac{\partial^3 \tilde{V}}{\partial \eta^3} - \frac{\partial}{\partial \eta}\left(\frac{3\bar{T}'}{\bar{T}^2} \right) \frac{\partial^2 \tilde{V}}{\partial \eta^2} - \frac{\partial^2}{\partial \eta^2}\left(\frac{\bar{T}'}{\bar{T}^2} \right) \frac{\partial \tilde{V}}{\partial \eta} - \frac{\partial^3 W_3}{\partial \eta^3}$$

$$+\tilde{k}^2 \bar{T}^2 \left\{ \frac{2\tilde{\mu}}{\bar{\mu}} \bar{T}' + \frac{\bar{T}\eta}{\bar{\mu}} + \frac{\bar{T}'}{\bar{T}} + \frac{\bar{T}'}{\tilde{k}^2 \bar{\mu} \bar{T}^2} \right\} \bar{W} + \frac{2x\bar{T}}{\bar{\mu}} \frac{\partial^2 W_3}{\partial x \partial \eta} - 2x \frac{\bar{T}'}{\bar{\mu}} \frac{\partial W_3}{\partial x},$$

$$a_6 = -\frac{\tilde{k}^2 \bar{T}^2}{\bar{\mu}} 2x\eta \frac{\partial \tilde{\theta}}{\partial x}, \quad a_7 = -2x\bar{T}\tilde{k}^2 \frac{\partial^2 \tilde{\theta}}{\partial \eta \partial x},$$

$$a_8 = \left\{ \frac{3\bar{T}'}{\bar{T}} - \frac{\eta \bar{T}}{\bar{\mu}} - \frac{2\tilde{\mu}}{\bar{\mu}} \bar{T}\bar{T}' \right\} \frac{\partial^2 \bar{W}}{\partial \eta^2},$$

$$a_9 = \left\{ 2\bar{T}^2 \tilde{k}^2 + \frac{\eta \bar{T}' + 2\bar{T}}{\bar{\mu}} + \left(\frac{\tilde{\mu}}{\bar{\mu}} - \frac{1}{\bar{T}} \right) \left(\frac{3\bar{T}'^2}{\bar{T}} - \bar{T}'' \right) - \frac{\tilde{\mu}'}{\bar{\mu}} \bar{T}' \right\} \frac{\partial \bar{W}}{\partial \eta}.$$

In these equations, W_3 and $\bar{W}$ are given by

$$W_3 = \frac{\bar{\mu}}{\sigma \bar{T}^2} \frac{\partial^2 \tilde{\theta}}{\partial \eta^2} + \left(\frac{2\tilde{\mu}\bar{T}'}{\sigma \bar{T}^2} - \frac{\bar{\mu}\bar{T}'}{\sigma \bar{T}^3} \right) \frac{\partial \tilde{\theta}}{\partial \eta} + \left\{ \frac{1}{\sigma \bar{T}} \frac{\partial}{\partial \eta} \left(\frac{\tilde{\mu}\bar{T}'}{\bar{T}} \right) - \frac{\bar{\mu}}{\sigma} \tilde{k}^2 \right\} \tilde{\theta},$$

$$\bar{W} = -\frac{1}{\bar{T}} \frac{\partial \tilde{V}}{\partial \eta} + W_3.$$

Appendix C. Expressions for b_i appearing in (6.9)

$$a_1 = \frac{4\tilde{T}'}{\tilde{T}} \frac{\partial^3 \tilde{V}}{\partial Y^3} + \left(\frac{6\tilde{T}''}{\tilde{T}} - \frac{12\tilde{T}'^2}{\tilde{T}^2} + \tilde{k}^2 \tilde{T}^2 \right) \frac{\partial^2 \tilde{V}}{\partial \tilde{T}^2}$$

$$+ \left(\frac{4\tilde{T}^{(3)}}{\tilde{T}} - \frac{24\tilde{T}''\tilde{T}'}{\tilde{T}^2} + \frac{24\tilde{T}'^3}{\tilde{T}^3} - \tilde{k}^2 \tilde{T}\tilde{T}' + \frac{F}{1+\tilde{m}} \tilde{k}^2 \tilde{T}^{5/2} \right) \frac{\partial \tilde{V}}{\partial Y}$$

$$+ \left(\frac{\tilde{T}^{(4)}}{\tilde{T}} - \frac{8\tilde{T}^{(3)}\tilde{T}'}{\tilde{T}^2} + \frac{36\tilde{T}''\tilde{T}'^2}{\tilde{T}^3} - \frac{6\tilde{T}''^2}{\tilde{T}^2} - \frac{24\tilde{T}'^4}{\tilde{T}^4} + \frac{3}{4}\tilde{k}^2 \tilde{T}'^2 \right.$$

$$\left. -\tfrac{1}{2}\tilde{k}^2 \tilde{T}\tilde{T}'' - \tilde{k}^4 \tilde{T}^4 + \frac{\tilde{k}^2 \tilde{T}^{3/2}}{1+\tilde{m}} (\tilde{T}' F - F'' \Omega) \right) \tilde{V},$$

$$a_2 = \tilde{T}\frac{\partial^3 W_3}{\partial Y^3} + \left(\frac{\tilde{T}'F'}{\tilde{T}} - F''\right)\frac{\tilde{T}^{3/2}}{1+\tilde{m}}(2x)\frac{\partial W_3}{\partial x} - \frac{F'\tilde{T}^{3/2}}{1+\tilde{m}}(2x)\frac{\partial^2 W_3}{\partial x \partial Y}$$
$$+\left[\frac{\tilde{T}^{3/2}F''}{1+\tilde{m}} - \frac{F'\tilde{T}'\sqrt{\tilde{T}}}{1+\tilde{m}} - \tilde{k}^2\tilde{T}^2\tilde{T}'\right]\bar{W} + \left(\frac{F\tilde{T}^{3/2}}{1+\tilde{m}} - 2\tilde{T}'\right)\frac{\partial^2 \bar{W}}{\partial Y^2}$$
$$-\left[\frac{F\tilde{T}'\sqrt{\tilde{T}} - 2F'\tilde{T}^{3/2}}{1+\tilde{m}} - \frac{5\tilde{T}'^2}{4\tilde{T}} + \tfrac{1}{2}\tilde{T}'' + \tilde{k}^2\tilde{T}^3\right]\frac{\partial \bar{W}}{\partial Y},$$

$$a_3 = \left[\frac{F''}{\tilde{T}}\Omega^2 + \left(F' - \frac{\tilde{T}'F}{\tilde{T}}\right)\Omega - \tilde{T}F - \tilde{G}F' + \tfrac{1}{2}(1+\tilde{m})\left(\frac{\tilde{T}'}{\sqrt{\tilde{T}}} + \frac{\Omega\tilde{T}''}{\tilde{T}^{3/2}} - \frac{3\Omega\tilde{T}'^2}{2\tilde{T}^{5/2}}\right)\right]$$
$$\times\frac{\tilde{k}^2\tilde{T}^{5/2}\tilde{U}}{(1+\tilde{m})\sqrt{2x}} + \frac{\Omega\tilde{T}'}{2\sqrt{2x}}\tilde{k}^2\tilde{T}\frac{\partial\tilde{U}}{\partial Y} - \tfrac{1}{2}\tilde{k}^2\tilde{T}^2\tilde{T}'\sqrt{2x}\frac{\partial\tilde{U}}{\partial x},$$

$$a_4 = \left\{\frac{1}{1+\tilde{m}}[\tfrac{1}{2}\tilde{G}F'^2 + \tilde{T}FF' + \tilde{T}'F^2 - (F'^2 + FF'')\Omega]\right.$$
$$\left.+\frac{F^{(3)}\Omega}{2\sqrt{\tilde{T}}} + \tfrac{1}{2}\sqrt{\tilde{T}}F'' - \frac{3F''\Omega\tilde{T}'}{4\tilde{T}^{3/2}} - \frac{\tilde{T}''F + \tilde{T}'F'}{\sqrt{\tilde{T}}} + \frac{3F\tilde{T}'^2}{2\tilde{T}^{3/2}}\right\}\tilde{k}^2\tilde{T}^{3/2}\frac{\tilde{\theta}}{\sqrt{2x}}$$
$$+\frac{1}{\sqrt{2x}}\tilde{k}^2\tilde{T}(\tfrac{1}{2}F''\Omega - F\tilde{T}')\frac{\partial\tilde{\theta}}{\partial Y} + \tfrac{1}{2}\tilde{k}^2\tilde{T}^2F''\sqrt{2x}\frac{\partial\tilde{\theta}}{\partial x}.$$

In these equations, $\bar{W}$ and W_3 are given by

$$W_3 = \frac{\Omega}{\sqrt{2x}\,\tilde{T}}\frac{\partial\tilde{U}}{\partial Y} - \frac{F}{\sqrt{2x}\,\tilde{T}}\frac{\partial\tilde{\theta}}{\partial Y} - \sqrt{2x}\frac{\partial\tilde{U}}{\partial x} + \frac{F'}{\tilde{T}}\sqrt{2x}\frac{\partial\tilde{\theta}}{\partial x} - \frac{\Omega\tilde{T}'}{\sqrt{2x}\,\tilde{T}^2}\tilde{U} + \frac{F\tilde{T}'}{\sqrt{2x}\,\tilde{T}^2}\tilde{\theta},$$

$$\bar{W} = -\frac{1}{\tilde{T}}\frac{\partial\tilde{V}}{\partial Y} + \frac{\tilde{T}'}{\tilde{T}^2}\tilde{V} + W_3.$$

References

Becker, E. 1968 *Gas dynamics*. New York and London: Academic Press.

Blackaby, N. D., Hall, P. & Cowley, S. J. 1993 On the instability of hypersonic flow past a flat plate. *J. Fluid Mech.* (In the press.)

Buddenberg, J. W. & Wilke, J. R. 1949 Calculation of gas mixture viscosities. *Indust. Engng Chem.* **41**, 1345-1347.

Chapman, S. & Cowling, T. G. 1970 *The mathematical theory of non-uniform gases*, 3rd edn. Cambridge University Press.

Cowley, S. & Hall, P. 1990 On the instability of hypersonic flow past a wedge. *J. Fluid Mech.* **214**, 17.

Denier, J. P., Hall, P. & Seddougui, S. 1990 On the receptivity problem for Görtler vortices: vortex motions induced by wall roughness. *Phil. Trans. R. Soc. Lond.* A **335**, 51-85.

Freeman, N. C. & Lam, S. H. 1959 On the Mach number independence principle for a hypersonic boundary layer. Princeton University Report 471.

Hall, P. 1982 Taylor–Görtler vortices in fully developed or boundary layer flows: linear theory. *J. Fluid Mech.* **124**, 475-494.

Hall, P. 1983 The linear development of Görtler vortices in growing boundary layers. *J. Fluid Mech.* **130**, 41-57.

Hall, P. 1988 The nonlinear development of Görtler vortices in growing boundary layers. *J. Fluid Mech.* **193**, 243.

Hall, P. 1990 Görtler vortices in growing boundary layers: the leading edge receptivity problem, linear growth and the nonlinear breakdown stage. *Mathematika* **37**, 151-189.

Hall, P. & Fu, Y. B. 1989 On the Görtler vortex instability mechanism at hypersonic speeds. *Theor. comput. Fluid Dynamics* **1**, 125-134.

Hall, P. & Malik, M. R. 1987 Görtler vortices in compressible boundary layers. *J. Engng Math.* **23**, 239.

Hall, P. & Smith, F. T. 1991 On strongly nonlinear vortex/wave interactions in boundary-layer transition. *J. Fluid Mech.* **227**, 641-666.

Lighthill, M. J. 1957 Dynamics of a dissociating gas. I. Equilibrium flow. *J. Fluid Mech.* **2**, 1-32.

Lindsay, A. L. & Bromley, L. A. 1950 Thermal conductivity of gas mixtures. *Indust. Engng Chem.* **42**, 1508-1511.

Mack, L. M. 1984 Boundary layer stability theory. AGARD report 709.

Seddougui, S. O., Bowles, R. I. & Smith, F. T. 1991 Surface-cooling effects on compressible boundary-layer instability. *Eur. J. Mech.* B **10**, 117–145.

Smith, F. T. 1989 On the first-mode instability in subsonic, supersonic or hypersonic boundary layers. *J. Fluid Mech.* **198**, 127-153.

Smith, F. T. & Brown, S. N. 1990 The inviscid instability of a Blasius boundary layer at large values of the Mach number. *J. Fluid Mech.* **219**, 499.

Spall, R. E. & Malik, M. R. 1989 Görtler vortices in supersonic and hypersonic boundary layers. *Phys. Fluids* A **1**, 1822.

Stewartson, K. 1964 *The theory of laminar boundary layers in compressible flows.* Oxford: Clarendon Press.

Wadey, P. 1993 Görtler vortices in compressible boundary layers. (Ph.D. thesis, Exeter University, U.K.) *Eur. J. Mech.* (In the press.)

Received 12 June 1991; revised 6 March 1992; accepted 22 May 1992

PHILOSOPHICAL TRANSACTIONS OF THE ROYAL SOCIETY A MATHEMATICAL, PHYSICAL & ENGINEERING SCIENCES